Available online at www.sciencedirect.com
ScienceDirect
Comput. Methods Appl. Mech. Engrg. 327 (2017) 173–195
Computer methods in applied mechanics and engineering
www.elsevier.com/locate/cma

Virtual Element approximation of 2D magnetostatic problems

L. Beirão da Veiga[a,b], F. Brezzi[b,*], F. Dassi[a], L.D. Marini[c,b], A. Russo[a,b]

[a] *Dipartimento di Matematica e Applicazioni, Università di Milano–Bicocca, Via Cozzi 53, I-20153, Milano, Italy*
[b] *IMATI CNR, Via Ferrata 1, I-27100 Pavia, Italy*
[c] *Dipartimento di Matematica, Università di Pavia, Via Ferrata 5, I-27100 Pavia, Italy*

Available online 1 September 2017

Abstract

We consider the use of nodal and edge Virtual Element spaces for the discretization of magnetostatic problems in two dimensions, following the variational formulation of Kikuchi. In addition, we present a novel Serendipity variant of the same spaces that allow to save many internal degrees of freedom. These Virtual Element Spaces of different type can be useful in applications where an exact sequence is particularly convenient, together with commuting-diagram interpolation operators, as is definitely the case in electromagnetic problems. We prove stability and optimal error estimates, and we check the performance with some academic numerical experiments.

MSC 2010: 65N30
Keywords: Finite Element Methods; Virtual Element Methods; Magnetostatic problems; Serendipity

1. Introduction

This paper is a first step towards the application of the Virtual Element technology, VEM, (see e.g. [1–3]) to the numerical solution of Electromagnetic problems.

Virtual Elements, introduced in [1], originate from the Mimetic Finite Difference methods, MFD, (see for instance [4–8] and the references therein), and their main difference with respect to MFD is that, instead of dealing only with degrees of freedom (as in classical Finite Differences), Virtual Elements deal with subspaces of the infinite dimensional spaces, in the traditional framework of Galerkin methods.

Presently, VEMs can be seen as being part of the wider family of Galerkin methods based on decompositions of the computational domains in polygons or polyhedrons, as Discontinuous Galerkin (see e.g. [9–11], or recently [12], and the references therein) or Hybridizable Discontinuous Galerkin and their variants (see for instance [13,14], or the much more recent [15] and the references therein) based on one or more local polynomial spaces. But one could also take into account that VEMs deal, in fact, with non-polynomial basis functions and should, in this respect,

* Corresponding author.
E-mail addresses: lourenco.beirao@unimib.it (L. Beirão da Veiga), brezzi@imati.cnr.it (F. Brezzi), franco.dassi@unimib.it (F. Dassi), marini@imati.cnr.it (L.D. Marini), alessandro.russo@unimib.it (A. Russo).

http://dx.doi.org/10.1016/j.cma.2017.08.013

be related more to other methods such as polygonal interpolant basis functions, barycentric coordinates, mean value coordinates, metric coordinate method, natural neighbor-based coordinates, generalized FEMs, and maximum entropy shape functions. See for instance [16–24], and the references therein.

Finally, many aspects are closely connected with Finite Volumes and related methods (see for instance [25–28] and the references therein).

A very brief list of VEMs applied to different types of problems is [29–36].

Here we consider the simplest case of Magnetostatic two-dimensional problem:

$$\begin{cases} \text{given } j \in L^2(\Omega) \quad \left(\text{with } \displaystyle\int_\Omega j \, \mathrm{d}\Omega = 0\right), \quad \text{and } \mu \in \mathbb{R}, \\ \text{find } \boldsymbol{H} \in H(\mathrm{rot};\, \Omega) \text{ and } \boldsymbol{B} \in H(\mathrm{div};\, \Omega) \text{ such that:} \\ \mathrm{rot}\, \boldsymbol{H} = j \text{ and } \mathrm{div}\, \boldsymbol{B} = 0, \text{ with } \boldsymbol{B} = \mu \boldsymbol{H}, \text{ in } \Omega \\ \text{with the boundary conditions } \boldsymbol{H} \cdot \boldsymbol{t} = 0 \text{ on } \partial\Omega \end{cases} \tag{1.1}$$

where $\Omega \subset \mathbb{R}^2$ is a simply connected polygon, and $\mathrm{rot}\, \boldsymbol{v} := \frac{\partial v_2}{\partial x} - \frac{\partial v_1}{\partial y}$. It is clear that (1.1) could be easily reduced to a simple elliptic problem, and even to a Poisson problem for a constant permeability μ, just by introducing a scalar variable A (potential) such that $A_x = B_2$, $A_y = -B_1$. In fact, it is easy to check that the function A is the solution of the Poisson problem

$$\begin{cases} -\mathrm{div}\,(\mu^{-1} \nabla A) = j & \text{in } \Omega \\ \dfrac{\partial A}{\partial n} = 0 & \text{on } \partial\Omega. \end{cases} \tag{1.2}$$

Hence the interest of (1.1), in itself, is surely minor. However, as we shall see, the purpose here is to set the way to the three-dimensional case (and in particular to the combined use of Serendipity-nodal and Serendipity-edge virtual elements to be used on the *faces* of a polyhedral decomposition).

We recall that, strictly sticking to the two-dimensional case, the use of Serendipity elements would not be particularly relevant, since a similar effect (i.e., to get rid of the internal degrees of freedom) could be obtained by the usual *static condensation*. But this will not be the case when the two-dimensional Serendipity elements are used on the faces of a three-dimensional decomposition, where standard static condensation could not be used, and even sophisticated techniques in reordering the unknowns during a Gaussian elimination could not be as effective as a direct Serendipity approach.

With this in mind, here we will study the numerical solution of (1.1) using the natural restriction to the two-dimensional case of the variational formulation of Kikuchi (introduced for the three-dimensional case in [37,38]). As we said, in order to reduce the number of *internal* degrees of freedom, we will give particular attention to the use of Serendipity variants. Serendipity VEMs were already introduced, in [39] for nodal elements, and in [40] for edge/face elements. However, the Serendipity elements presented here *do not* coincide with those defined in [39] and in [40], since the local projectors use different degrees of freedom. Actually, as we shall see in more details in Sections 5 and 6, the Serendipity elements defined in [39] and in [40] would **not** give rise to the necessary exact sequence for our two-dimensional problem (1.1), and also on the faces of three dimensional problems, while the present ones have been tailored specifically for that purpose.

To give, in advance, an idea of the relevance that the use of Serendipity VEMs on faces could have, we anticipate here a schematic three dimensional example about this gain. For the sake of simplicity, in order to clarify the order of magnitude of the gain, in Tables 1 and 2 we compared the number of **inter-element degrees of freedom** (vertices, edges, and faces) on some simple uniform meshes of cubes ($8 \times 8 \times 8$, $16 \times 16 \times 16$, and $32 \times 32 \times 32$), for $k = 2, 3, 4, 5$, without counting the degrees of freedom *internal* to the cubes, (assuming, in some sense, that all the degrees of freedom internal to the cubes were eliminated by standard static condensation).

For each decomposition, and for each value of k between 2 and 5, we compared the inter-element degrees of freedom needed when using **on all faces**: either standard nodal two dimensional $\mathbb{Q}_k$ finite elements, or our nodal two-dimensional Virtual Elements (VEM_k), or their present two-dimensional Serendipity variants ($\mathrm{VEM}\mathcal{S}_k$) . We point out that $\mathbb{Q}_k$ Finite Elements (on a schematic decomposition like this one) could also have efficient Serendipity variants (see e.g. [41,42]), that however would suffer losses of accuracy for more general decompositions (and already when using faces that are non-affine quadrilaterals).

A layout of the paper is as follows: in the next section we will introduce some basic notation, recall some well known properties of polynomial spaces, and present the Kikuchi formulation of (1.1). Then in Section 3 we present

Table 1
Number of inter-element dofs for cubic uniform mesh: $k = 2$ and $k = 3$.

Mesh	Interelement dofs $k = 2$			Mesh	Interelement dofs $k = 3$		
	VEM$\mathcal{S}_2$	VEM$_2$	$\mathbb{Q}_2$		VEM$\mathcal{S}_3$	VEM$_3$	$\mathbb{Q}_3$
8^3	2,673	7,857	4,401	8^3	4,617	14,985	11,529
16^3	18,785	57,953	31,841	16^3	32,657	110,993	84,881
32^3	140,481	444,609	241,857	32^3	245,025	853,281	650,529

Table 2
Number of inter-element dofs for cubic uniform mesh: $k = 4$ and $k = 5$.

Mesh	Interelement dofs $k = 4$			Mesh	Interelement dofs $k = 5$		
	VEM$\mathcal{S}_4$	VEM$_4$	$\mathbb{Q}_4$		VEM$\mathcal{S}_5$	VEM$_5$	$\mathbb{Q}_5$
8^3	8,289	23,841	22,113	8^3	15,417	34,425	36,153
16^3	59,585	177,089	164,033	16^3	112,625	256,241	269,297
32^3	450,945	1,363,329	1,261,953	32^3	859,617	1,974,753	2,076,129

the *local* Virtual Element spaces of nodal type and of edge type. As we mentioned already, *the spaces* are the same already discussed in [1,43] and in [3,44], respectively, but using *different* (though computationally equivalent) *degrees of freedom*, that will come handy for the Serendipity construction. In Section 4 we present the *global* version of the Virtual Element spaces, use them to write the discretized problem, and prove the corresponding error bounds. In Section 5 we introduce and discuss the Serendipity variants, both for nodal and edge elements, and prove some crucial properties of the coupling of the two for the (simpler) case in which, for each element, the local order is smaller than the number of edges. Then, in Section 6, we briefly discuss the extension of the previous results to the case of VEMs of an order (locally) higher than (or equal to) the number of edges. In Section 7 we present some numerical results that show that the quality of the approximation is very good, and also that the Serendipity variant does not jeopardize the accuracy. Finally, in Section 9 we draw some conclusions.

2. Notation and variational formulation

2.1. Basic notation

In two dimensions, we will denote by $\boldsymbol{x}$ the independent variable, using $\boldsymbol{x} = (x, y)$ or (more often) $\boldsymbol{x} = (x_1, x_2)$ following the circumstances. We will also use $\boldsymbol{x}^\perp := (-x_2, x_1)$, and in general, for a vector $\boldsymbol{v} \equiv (v_1, v_2)$,

$$\boldsymbol{v}^\perp := (-v_2, v_1). \tag{2.1}$$

Moreover, for a vector $\boldsymbol{v}$ and a scalar q we will write

$$\mathrm{rot}\, \boldsymbol{v} := \frac{\partial v_2}{\partial x} - \frac{\partial v_1}{\partial y}, \qquad \mathbf{rot}\, q := \left(\frac{\partial q}{\partial y}, -\frac{\partial q}{\partial x}\right)^T \tag{2.2}$$

and we consider the spaces

$$H^1(\Omega) = \{q \in L^2(\Omega) \text{ with } \nabla q \in [L^2(\Omega)]^2\}, \tag{2.3}$$

$$H(\mathrm{rot};\, \Omega) = \{\boldsymbol{v} \in [L^2(\Omega)]^2 \text{ with } \mathrm{rot}\, \boldsymbol{v} \in L^2(\Omega)\}, \tag{2.4}$$

and for taking into account boundary conditions

$$H^1_0(\Omega) = \{q \in H^1(\Omega) \text{ with } q = 0 \text{ on } \partial\Omega\}, \tag{2.5}$$

$$H_0(\mathrm{rot};\, \Omega) = \{\boldsymbol{v} \in H(\mathrm{rot};\, \Omega) \text{ with } \boldsymbol{v} \cdot \boldsymbol{t} = 0 \text{ on } \partial\Omega\}, \tag{2.6}$$

where $\boldsymbol{t}$ denotes the unit tangent vector. For an integer $s \geq -1$ we denote by $\mathbb{P}_s$ the space of polynomials of degree $\leq s$. Following a common convention, $\mathbb{P}_{-1} \equiv \{0\}$ and $\mathbb{P}_0 \equiv \mathbb{R}$. Moreover, for $s \geq 1$, on a domain $\mathcal{O}$,

$$\mathbb{P}_s^0(\mathcal{O}) := \{q \in \mathbb{P}_s \text{ such that } \int_{\mathcal{O}} q \, \mathrm{d}\mathcal{O} = 0\}. \tag{2.7}$$

We denote by $\pi_{s,d}$ (here for $d = 1$ or $d = 2$) the dimension of $\mathbb{P}_s$ in d space dimensions, and we recall that

$$\pi_{s,1} = s + 1 \qquad \text{and} \qquad \pi_{s,2} = (s + 1)(s + 2)/2. \tag{2.8}$$

Obviously, in d dimensions, the (common value) of the dimension of the space $\mathbb{P}_s^0$ and of the spaces $\nabla(\mathbb{P}_s)$, $\mathbf{rot}\,(\mathbb{P}_s)$ will be equal to the dimension of $\mathbb{P}_s$ minus one.

The following decompositions are well known:

$$(\mathbb{P}_s)^2 = \mathbf{rot}\,\mathbb{P}_{s+1} \oplus \boldsymbol{x}\mathbb{P}_{s-1} \quad \text{and} \quad (\mathbb{P}_s)^2 = \mathbf{grad}\,\mathbb{P}_{s+1} \oplus \boldsymbol{x}^{\perp}\mathbb{P}_{s-1}, \tag{2.9}$$

implying that

$$\text{div} \text{ is an isomorphism between } \left\{\boldsymbol{x}\mathbb{P}_s\right\} \text{ and } \mathbb{P}_s, \tag{2.10}$$

$$\text{rot} \text{ is an isomorphism between } \left\{\boldsymbol{x}^{\perp}\mathbb{P}_s\right\} \text{ and } \mathbb{P}_s. \tag{2.11}$$

Finally we recall the definition of the classical *local* spaces for mixed formulations

$$RT_s = \mathbf{rot}\,\mathbb{P}_{s+1} \oplus \boldsymbol{x}\mathbb{P}_s \text{ and } N1_s = \mathbf{grad}\,\mathbb{P}_{s+1} \oplus \boldsymbol{x}^{\perp}\mathbb{P}_s \tag{2.12}$$

and

$$BDM_s \equiv N2_s := (\mathbb{P}_s)^2. \tag{2.13}$$

2.2. Computationally equivalent sets of degrees of freedom

As we shall see, we are going to deal in each element with finite dimensional spaces whose functions are defined as the solution of a boundary value problem within the element. The problem will be individuated by a certain number of parameters that will then be used, in the actual computations, as *degrees of freedom*. As the local dimension (as we said) will always be finite, it is clear that, on the one hand, an arbitrary set of n (= dimension of the local space) linearly independent functionals will constitute a *unisolvent set of degrees of freedom*, and consequently all such sets could be considered as *equivalent*, as they identify the same finite dimensional space. On the other hand, starting from the values of a set of n functionals there will be *some* other quantities that can be computed, out of them, without solving the boundary value problem: as, trivially, if we give the sum and the difference of two numbers instead of the two number themselves, or, a little less trivially, if we give the mean value of the normal derivative of a smooth function on the boundary of the element and we want to compute the mean value of its Laplacian in the same element. Hence, we will say that two sets of degrees of freedom $(\delta_1, \ldots, \delta_n)$ and $(\zeta_1, \ldots, \zeta_n)$ are **computationally equivalent** if one can compute one set out of the other, on the computer, with simple algebraic manipulations *without solving the boundary value problem*. As a negative example, consider the one-dimensional linear space of functions $u \in H_0^1(E)$ such that $\Delta u =$ constant. This space can be described by assigning either the constant value of Δu or the mean value of u. However, these degrees of freedom are *not computationally equivalent*, since in general we cannot compute one out of the other without solving a PDE in E.

2.3. The variational formulation

Among the various possible variational formulations of (1.1) we will consider the *K-formulation* introduced in [37] and [38], that reads

$$\begin{cases} \text{find } \boldsymbol{H} \in H_0(\mathrm{rot};\, \Omega) \text{ and } p \in H_0^1(\Omega) \text{ such that:} \\ \displaystyle\int_{\Omega} \mathrm{rot}\, \boldsymbol{H}\, \mathrm{rot}\, \boldsymbol{v}\, \mathrm{d}\Omega + \int_{\Omega} \nabla p \cdot \mu \boldsymbol{v}\, \mathrm{d}\Omega = \int_{\Omega} j\, \mathrm{rot}\, \boldsymbol{v}\, \mathrm{d}\Omega \quad \forall \boldsymbol{v} \in H_0(\mathrm{rot};\, \Omega) \\ \displaystyle\int_{\Omega} \nabla q \cdot \mu \boldsymbol{H}\, \mathrm{d}\Omega = 0 \quad \forall q \in H_0^1(\Omega). \end{cases} \tag{2.14}$$

It is easy to check, by the usual theory of mixed methods (see e.g. [45]), that (2.14) has a unique solution $(\boldsymbol{H}, p)$. Then we check that $p \equiv 0$ and that $\boldsymbol{H}$ and $\boldsymbol{B} \equiv \mu\boldsymbol{H}$ give the solution of (1.1). Indeed, checking that $p \equiv 0$ is immediate, just taking $\boldsymbol{v} = \nabla p$ in the first equation; and once we know that $p \equiv 0$ the first equation gives rot $\boldsymbol{H} = j$, and then the second equation gives div $\mu\boldsymbol{H} = 0$.

It should be pointed out that problem (2.14) has also an equivalent formulation of the *Hodge–Laplacian* type, [46], that however will not be dealt with here. Other boundary conditions could be easily considered as well. Needless to say, there are a number of different (and much more general) ways to tackle electromagnetic problems. We briefly refer, for instance, to [47], [48,49] and to the references therein. Theoretical results more related to the present approach can be found in [50,51].

3. The local VEM spaces

We will now design a Virtual Element approximation of (2.14), taking into account different possible variants for the space of *scalar multipliers* as well as for the H(rot)-conforming vectors.

Later on, these same spaces will be reduced with a Serendipity approach, in order to eliminate as many internal degrees of freedom as possible. This will come out as particularly relevant in future developments concerning the three-dimensional problems, when the elements of the present papers will have to be used on *faces*, where the use of static condensation would be much more involved.

We begin by defining the local spaces to be used for the approximation. We assume therefore that E is a generic polygon, with N_e edges e, satisfying the usual regularity assumptions (see, e.g., [1]).

3.1. The local spaces—nodal

We recall here the definition of the local nodal spaces. Actually, the spaces presented here are exactly the same as the ones in [1], but with different (though *computationally equivalent*) degrees of freedom.

Let k, k_d be integers with $k \geq 1$. For k_d we will consider, in principle, the three cases $k-2 \leq k_d \leq k$. For the **nodal** spaces we have,

$$V_k^n(E) := \left\{ q \in C^0(\overline{E}) : \ q_{|e} \in \mathbb{P}_k(e) \ \forall e \in \partial E, \ \Delta q \in \mathbb{P}_{k_d}(E) \right\}, \tag{3.1}$$

with the degrees of freedom

- the nodal values $q(v)$ at all vertices v of E, (3.2)
- for each edge e, the moments $\displaystyle\int_e q \ p_{k-2} \, \mathrm{d}s \quad \forall p_{k-2} \in \mathbb{P}_{k-2}(e)$, (3.3)
- $\displaystyle\int_E (\nabla q \cdot \boldsymbol{x}_{\mathrm{E}}) \ p_{k_d} \, \mathrm{d}E \quad \forall p_{k_d} \in \mathbb{P}_{k_d}(E)$, (3.4)

where $\boldsymbol{x}_{\mathrm{E}} = \boldsymbol{x} - \mathbf{b}_{\mathrm{E}}$, with $\mathbf{b}_{\mathrm{E}} =$ barycenter of E.

Proposition 3.1. *The degrees of freedom (3.2)–(3.4) are unisolvent.*

Proof. The number of conditions being equal to the dimension of $V_k^n(E)$ (as they are both equal to $N_e \, \pi_{k-1,1} + \pi_{k_d,2}$) we have to prove that if, for a certain $q \in V_k^n(E)$, all the d.o.f. vanish, then $q \equiv 0$. Setting to zero the values of the degrees of freedom (3.2)–(3.3) gives immediately

$$q \equiv 0 \text{ on } \partial E, \tag{3.5}$$

which, setting to zero (3.4) as well, implies

$$0 = \int_E (\nabla q \cdot \boldsymbol{x}_{\mathrm{E}}) \ p_{k_d} \, \mathrm{d}E = -\int_E q \ \mathrm{div}\,(\boldsymbol{x}_{\mathrm{E}} \ p_{k_d}) \, \mathrm{d}E \quad \forall p_{k_d} \in \mathbb{P}_{k_d}. \tag{3.6}$$

Eq. (3.6), in view of (2.10), immediately implies

$$0 = \int_E q \ p_{k_d} \, \mathrm{d}E \quad \forall p_{k_d} \in \mathbb{P}_{k_d}. \tag{3.7}$$

Consequently, using (3.7) (plus the fact that $\Delta q \in \mathbb{P}_{k_d}$) and (3.5),we have:

$$\int_E |\nabla q|^2 \, \mathrm{d}E = -\int_E q \, \Delta q \, \mathrm{d}E + \int_{\partial E} q(\nabla q \cdot \boldsymbol{n}) \, \mathrm{d}s = 0, \tag{3.8}$$

and the proof is concluded. □

Remark 1. Looking at the proof above, one can easily see that the degrees of freedom (3.4), when used in conjunction with the usual boundary degrees of freedom (3.2)–(3.3), are computationally equivalent to the original degrees of freedom introduced in [1]:

$$\int_E q \, p_{k_d} \, \mathrm{d}E \qquad \forall p_{k_d} \in \mathbb{P}_{k_d}. \tag{3.9}$$

We also point out that the use of the degrees of freedom (3.4) is not much more complicated, computationally, than that of (3.9). □

Proposition 3.2. *For every $q \in V_k^n(E)$, using the degrees of freedom (3.2)–(3.4) one can compute the L^2-orthogonal projection of ∇q onto $[\mathbb{P}_{k_d+1}(E)]^2$.*

Proof. It is enough to observe that for every $q \in V_k^n(E)$ and for every $\boldsymbol{p}_{k_d+1} \in [\mathbb{P}_{k_d+1}(E)]^2$, integrating by parts we have

$$\int_E \Pi^0_{k_d+1} \nabla q \cdot \boldsymbol{p}_{k_d+1} \, \mathrm{d}E := \int_E \nabla q \cdot \boldsymbol{p}_{k_d+1} \, \mathrm{d}E = \int_{\partial E} q \, \boldsymbol{p}_{k_d+1} \cdot \boldsymbol{n} \, \mathrm{d}s - \int_E q \, \mathrm{div} \, \boldsymbol{p}_{k_d+1} \, \mathrm{d}E,$$

and all the terms in the right-hand side are computable (using in particular the equivalent dofs (3.9)). □

3.2. The local spaces—edge

We introduce now the local edge spaces. Once more, the spaces presented here are exactly the same already introduced in [3], but with different (though *computationally equivalent*) degrees of freedom.

For the edge spaces we will keep the same integers k and k_d of the nodal spaces, but here we have an additional integer parameter (that we call k_r) that in practice might assume the values $k-1$ or $k-2$ according to the type of approximation that we are willing to obtain. Roughly speaking, choosing $k_r = k-1$ we will get, for our edge space, a generalization to polygons of the *Nédélec elements of the first kind* $N1$ (that, in turn, in two dimension can be seen as *rotated Raviart–Thomas* spaces). Choosing instead $k_r = k-2$ we will get, for our edge space, a generalization to polygons of the *Nédélec elements of the second kind* $N2$ (that, in turn, in two dimension can be seen as *rotated Brezzi–Douglas–Marini* spaces); see also (2.12)–(2.13).

For the **edge** spaces we have then, for k and k_d as in the previous subsection, and for $k_r = k-1$ or (only when $k \geq 2$) for $k_r = k-2$:

$$V^e_{k-1}(E) := \Big\{ \boldsymbol{v} \in [L^2(E)]^2 \ : \ \mathrm{div} \, \boldsymbol{v} \in \mathbb{P}_{k_d}(E), \ \mathrm{rot} \, \boldsymbol{v} \in \mathbb{P}_{k_r}(E), \boldsymbol{v}_{|e} \cdot \boldsymbol{t}_e \in \mathbb{P}_{k-1}(e) \, \forall e \in \partial E \Big\}, \tag{3.10}$$

with the degrees of freedom

- on each $e \in \partial E$, the moments $\displaystyle\int_e (\boldsymbol{v} \cdot \boldsymbol{t}_e) p_{k-1} \, \mathrm{d}s \ \forall p_{k-1} \in \mathbb{P}_{k-1}(e)$, (3.11)
- the moments $\displaystyle\int_E \boldsymbol{v} \cdot \boldsymbol{x}_{\mathrm{E}} \, p_{k_d} \, \mathrm{d}E \quad \forall p_{k_d} \in \mathbb{P}_{k_d}(E)$, (3.12)
- $\displaystyle\int_E \mathrm{rot} \, \boldsymbol{v} \, p^0_{k_r} \, \mathrm{d}E \quad \forall p^0_{k_r} \in \mathbb{P}^0_{k_r}(E) \qquad (\text{only for } k_r > 0)$, (3.13)

where $\mathbb{P}^0_s$ was defined in (2.7).

Proposition 3.3. *The degrees of freedom (3.11)–(3.13) are unisolvent.*

Proof. Since the number of d.o.f. equals the dimension of $V^e_{k-1}(E)$ (as they are both equal to $N_e\pi_{k-1,1} + \pi_{k_d,2} + \pi_{k_r,2} - 1$), we have to prove that if, for a certain $\boldsymbol{v} \in V^e_{k-1}(E)$, all the d.o.f. vanish, then $\boldsymbol{v} \equiv 0$. Conditions (3.11), set equal to zero, give $\boldsymbol{v} \cdot \boldsymbol{t} = 0$ on ∂E, and hence

$$\int_E \mathrm{rot}\, \boldsymbol{v}\ \mathrm{d}E = 0.$$

This, together with the d.o.f. (3.13) set to be zero, implies

$$\mathrm{rot}\, \boldsymbol{v} = 0.$$

In view of (2.10) there exists a unique $p^* \in \mathbb{P}_{k_d}$ such that $\mathrm{div}\,(\boldsymbol{v} - \boldsymbol{x}_{\mathrm{E}} p^*) = 0$ and therefore $\boldsymbol{v} - \boldsymbol{x}_{\mathrm{E}} p^* = \mathbf{rot}\, \varphi$ for some $\varphi \in H^1(E)$. Then, if the d.o.f. (3.12) are also zero, integrating the remaining term by parts we have

$$\int_E |\boldsymbol{v}|^2\, \mathrm{d}E = \int_E \boldsymbol{v} \cdot (\boldsymbol{x}_{\mathrm{E}} p^* + \mathbf{rot}\, \varphi)\, \mathrm{d}E = 0 + \int_E \mathrm{rot}\, \boldsymbol{v}\, \varphi\, \mathrm{d}E + \int_{\partial E} \boldsymbol{v} \cdot \boldsymbol{t}\, \varphi\, \mathrm{d}s = 0,$$

and the proof is concluded. □

Note that

$$\mathbb{P}_k(E) \subseteq V^n_k(E), \text{ and } [\mathbb{P}_{k-1}(E)]^2 \subseteq V^e_{k-1}(E).$$

Moreover, for each $\boldsymbol{v} \in V^e_{k-1}(E)$, the polynomial $\mathrm{rot}\, \boldsymbol{v} \in \mathbb{P}_{k_r}(E)$ is uniquely defined (and computable) by the d.o.f. (3.11) and (3.13).

Remark 2. Here too we remark that the d.o.f. (3.13), when used together with (3.11) and (3.12), are computationally equivalent to the original ones introduced first in [44] (up to a rotation of $\pi/2$, in order to go, in 2 dimensions, from $H(\mathrm{div})$ to $H(\mathrm{rot})$-conforming spaces), and also to those used in [3]. □

Remark 3. We point out that for $k_d \geq k-2$ the L^2-projection $\Pi^0_{k-1} : V^e_{k-1}(E) \to [\mathbb{P}_{k-1}(E)]^2$ is also computable using the degrees of freedom (3.11)–(3.13). Indeed, for any $\mathbf{p}_{k-1} \in [\mathbb{P}_{k-1}(E)]^2$ we can use (2.9) and write

$$\mathbf{p}_{k-1} = \mathbf{rot}\ q_k + \boldsymbol{x}_{\mathrm{E}} q_{k-2}, \qquad \text{for some } q_k \in \mathbb{P}_k(E), \text{ and some } q_{k-2} \in \mathbb{P}_{k-2}(E).$$

Therefore, for any $\boldsymbol{v} \in V^e_{k-1}(E)$ and any $\mathbf{p}_{k-1} \in [\mathbb{P}_{k-1}(E)]^2$ we can write

$$\begin{aligned}\int_E \Pi^0_{k-1}\boldsymbol{v} \cdot \mathbf{p}_{k-1}\, \mathrm{d}E \ &:= \int_E \boldsymbol{v} \cdot \mathbf{p}_{k-1}\, \mathrm{d}E = \int_E \boldsymbol{v} \cdot (\mathbf{rot}\ q_k + \boldsymbol{x}_{\mathrm{E}} q_{k-2})\, \mathrm{d}E \\ &= \int_E (\mathrm{rot}\, \boldsymbol{v}) q_k\, \mathrm{d}E + \sum_{e \in \partial E} \int_e (\boldsymbol{v} \cdot \boldsymbol{t}) q_k\, \mathrm{d}s + \int_E \boldsymbol{v} \cdot \boldsymbol{x}_{\mathrm{E}} q_{k-2}\, \mathrm{d}E\end{aligned}$$

and it is immediate to check that each of the last three terms is computable. □

3.3. The local scalar product

Once we have the L^2-projection from $V^e_{k-1}(E)$ onto polynomials of degree $k-1$, we can define in $V^e_{k-1}(E)$ the usual VEM-like inner product

$$[\boldsymbol{v}, \boldsymbol{w}]_{e,E} := (\Pi^0_{k-1}\boldsymbol{v}, \Pi^0_{k-1}\boldsymbol{w})_{0,E} + S_E((I - \Pi^0_{k-1})\boldsymbol{v}, (I - \Pi^0_{k-1})\boldsymbol{w}), \tag{3.14}$$

where S_E, as already classical in VEMs frameworks, is any symmetric and positive definite bilinear form such that there exist two constants α_* and α^* for which

$$\alpha_*(\boldsymbol{v}, \boldsymbol{v})_{0,E} \leq [\boldsymbol{v}, \boldsymbol{v}]_{e,E} \leq \alpha^*(\boldsymbol{v}, \boldsymbol{v})_{0,E} \qquad \forall \boldsymbol{v} \in V^e_{k-1}(E). \tag{3.15}$$

See, e.g., [1] or [3], or also [52] for simple choices of S_E. Under usual suitable shape regularity assumptions (see [1,53,54]) one can prove that the constants α_* and α^* in the above formula can be made independent of the diameter h_E of E.

It is important to point out that

$$[\boldsymbol{v}, \mathbf{p}_{k-1}]_{e,E} \equiv (\boldsymbol{v}, \mathbf{p}_{k-1})_{0,E} \quad \forall \boldsymbol{v} \in V^e_{k-1}(E),\ \forall \mathbf{p}_{k-1} \in [\mathbb{P}_{k-1}(E)]^2. \tag{3.16}$$

4. Discretization of the magnetostatic problem (2.14)

4.1. The global VEM spaces

At this point, given a decomposition $\mathcal{T}_h$ of the computational domain Ω into polygons, with the usual regularity assumptions, we can define the *global spaces*:

$$V_k^n = \left\{ q \in H_0^1(\Omega) \,:\, q_{|E} \in V_k^n(E) \,\forall E \in \mathcal{T}_h \right\}, \tag{4.1}$$

$$V_{k-1}^e = \left\{ \boldsymbol{v} \in H_0(\mathrm{rot};\, \Omega) \,:\, \boldsymbol{v}_{|E} \in V_{k-1}^e(E) \,\forall E \in \mathcal{T}_h \right\}. \tag{4.2}$$

The (global) degrees of freedom associated to these spaces are the obvious ones that stem, as in standard Finite Elements, from the local ones described above.

It is easy to check (see e.g. [3]) that

$$\nabla V_k^n \equiv \{ \boldsymbol{v} \in V_{k-1}^e \text{ such that } \mathrm{rot}\, \boldsymbol{v} = 0 \}. \tag{4.3}$$

Introducing the additional space of *piecewise polynomials in $\mathbb{P}_{k_r}$ with global zero mean value*

$$V_{k_r}^E := \left\{ \gamma \in L^2(\Omega) \,:\, \gamma_{|E} \in \mathbb{P}_{k_r}(E) \,\forall E \in \mathcal{T}_h, \text{ and } \int_\Omega \gamma \, \mathrm{d}\Omega = 0 \right\}, \tag{4.4}$$

we also have:

Proposition 4.1. *With the above definitions we have*

$$rot V_{k-1}^e \equiv V_{k_r}^E. \tag{4.5}$$

Proof. Indeed, the inclusion $\mathrm{rot}\, V_{k-1}^e \subseteq V_{k_r}^E$ is obvious. Let us see the converse. Given a $\gamma \in V_{k_r}^E$ we can easily find a $\boldsymbol{w} \in [H_0^1(\Omega)]^2$ such that $\mathrm{rot}\, \boldsymbol{w} = \gamma$. Then we define $\boldsymbol{w}_I$ as the unique function in V_{k-1}^e that takes the same degrees of freedom values as $\boldsymbol{w}$. In other words we set, for all $E \in \mathcal{T}_h$,

$$\begin{cases} \displaystyle\int_e (\boldsymbol{w} - \boldsymbol{w}_I) \cdot \boldsymbol{t}_e \; p_{k-1} \, \mathrm{d}s = 0 \qquad \forall e \in \partial E \,, \forall p_{k-1} \in \mathbb{P}_{k-1}(e), \\ \displaystyle\int_E (\boldsymbol{w} - \boldsymbol{w}_I) \cdot \boldsymbol{x}_{\mathrm{E}} \; p_{k_d} \, \mathrm{d}E = 0 \quad \forall p_{k_d} \in \mathbb{P}_{k_d}(E), \\ \displaystyle\int_E \mathrm{rot}\, (\boldsymbol{w} - \boldsymbol{w}_I) \; p_{k_r}^0 \, \mathrm{d}E = 0 \quad \forall p_{k_r}^0 \in \mathbb{P}_{k_r}^0(E). \end{cases} \tag{4.6}$$

Joining the third of (4.6) with the first (used for $p_{k-1} \equiv 1$) one can now check that for all $E \in \mathcal{T}_h$ it holds

$$(\mathrm{rot}\, \boldsymbol{w}_I)|_E = \Pi_{k_r}^0 (\mathrm{rot}\, \boldsymbol{w})|_E = \Pi_{k_r}^0 \gamma|_E = \gamma|_E, \tag{4.7}$$

that proves the above assertion. □

Remark 4. As is well known, in general, for mixed formulations, properties (4.3) and (4.5) play a very important role in the analysis of the numerical methods, as well as (most of the times) in their performance. We point out that, for *dual* mixed formulations of Darcy problems (as the classical ones, based on $H(div)$-L^2 pairs) the analog of (4.5) (usually, with *face* spaces, and div instead of rot) is the critical property. Here, instead, for problems like (2.14), it will be property (4.3) that is more difficult to deal with, in particular when using Serendipity VEMs. □

From (3.14) we can also define a scalar product in V_{k-1}^e in the obvious way

$$[\boldsymbol{v}, \boldsymbol{w}]_e := \sum_{E \in \mathcal{T}_h} [\boldsymbol{v}, \boldsymbol{w}]_{e,E}, \tag{4.8}$$

and we note that

$$\alpha_*(\boldsymbol{v}, \boldsymbol{v})_{0,\Omega} \le [\boldsymbol{v}, \boldsymbol{v}]_e \le \alpha^*(\boldsymbol{v}, \boldsymbol{v})_{0,\Omega} \qquad \forall \boldsymbol{v} \in V_{k-1}^e. \tag{4.9}$$

We note that the scalar product (4.8) is also well defined in the *DG version of* V^e_{k-1}, namely

$$V^{e,DG}_{k-1} := \left\{ \boldsymbol{v} \in [L^2(\Omega)]^2 \,:\, \boldsymbol{v}_{|E} \in V^e_{k-1}(E)\ \forall E \in \mathcal{T}_h \right\}. \tag{4.10}$$

It is also important to point out that, using (3.16) we have

$$[\boldsymbol{v}, \boldsymbol{w}]_e = \sum_{E\in\mathcal{T}_h} [\boldsymbol{v}, \boldsymbol{w}]_{e,E} = \sum_{E\in\mathcal{T}_h} (\boldsymbol{v}, \boldsymbol{w})_{0,E} = \int_\Omega \boldsymbol{v}\cdot\boldsymbol{w}\,\mathrm{d}\Omega \qquad \forall \boldsymbol{w} \in V^e_{k-1}, \tag{4.11}$$

whenever $\boldsymbol{v}$ is in $[\mathbb{P}_{k-1}(E)]^2$ for each $E \in \mathcal{T}_h$. Finally, since (4.11) also holds when both $\boldsymbol{v}$ and $\boldsymbol{w}$ are piecewise polynomials of degree $\le k-1$, and taking them equal to each other we easily see that, necessarily,

$$\alpha_* \le 1 \le \alpha^* \tag{4.12}$$

in (4.9).

4.2. The discretized problem

Given $j \in L^2(\Omega)$, with $\int_\Omega j\,\mathrm{d}\Omega = 0$, we can finally introduce the **discretization** of (2.14)

$$\begin{cases} \text{find } \boldsymbol{H}_h \in V^e_{k-1} \text{ and } p_h \in V^n_k \text{ such that:} \\ \displaystyle\int_\Omega \mathrm{rot}\,\boldsymbol{H}_h\,\mathrm{rot}\,\boldsymbol{v}\,\mathrm{d}\Omega + [\nabla p_h, \mu\boldsymbol{v}]_e = \int_\Omega j\,\mathrm{rot}\,\boldsymbol{v}\,\mathrm{d}\Omega \quad \forall \boldsymbol{v} \in V^e_{k-1}, \\ [\nabla q, \mu\boldsymbol{H}_h]_e = 0 \quad \forall q \in V^n_k. \end{cases} \tag{4.13}$$

We recall that both $\mathrm{rot}\,\boldsymbol{H}_h$ and $\mathrm{rot}\,\boldsymbol{v}$ are computable polynomials in each polygon E, so that all the terms in (4.13) are computable.

Proposition 4.2. *Problem (4.13) has a unique solution* $(\boldsymbol{H}_h, p_h)$*, and* p_h *is always equal to zero.*

Proof. Taking $\boldsymbol{v} = \nabla p_h$ (as we did for the continuous problem (2.14)) in the first equation, and using (4.9) we easily obtain $p_h \equiv 0$ for (4.13) as well. To prove uniqueness of $\boldsymbol{H}_h$, set $j = 0$, and let $\overline{\boldsymbol{H}}_h$ be the solution of the homogeneous problem. From the first equation we deduce that $\mathrm{rot}\,\overline{\boldsymbol{H}}_h = 0$. Hence, from (4.3) we have $\overline{\boldsymbol{H}}_h = \mu\nabla q^*_h$ for some $q^*_h \in V^n_k$. The second equation gives then $\overline{\boldsymbol{H}}_h = 0$. □

Once we know that the solution is unique and $p_h = 0$, the first equation of (4.13) reads

$$\int_\Omega (\mathrm{rot}\,\boldsymbol{H}_h - j)\,\mathrm{rot}\,\boldsymbol{v}\,\mathrm{d}\Omega = 0 \quad \forall \boldsymbol{v} \in V^e_{k-1} \tag{4.14}$$

that, in view of (4.5) and the compatibility condition on j (that is, j has zero mean value in Ω), implies

$$\mathrm{rot}\,\boldsymbol{H}_h = \Pi^0_{k_r}\, j. \tag{4.15}$$

4.3. Error estimates

Let us bound the error $\boldsymbol{H} - \boldsymbol{H}_h$. We start by defining the interpolant $\boldsymbol{H}_I$ of $\boldsymbol{H}$ as in (4.6). Using (4.7) and (4.15) we immediately have that

$$\mathrm{rot}\,(\boldsymbol{H}_I - \boldsymbol{H}_h) = 0 \tag{4.16}$$

and therefore, from (4.3),

$$\boldsymbol{H}_I - \boldsymbol{H}_h = \mu\nabla q^*_h \text{ for some } q^*_h \in V^n_k. \tag{4.17}$$

On the other hand, using (4.9) we have

$$\alpha_* \|\boldsymbol{H}_I - \boldsymbol{H}_h\|^2_{0,\Omega} \le [\boldsymbol{H}_I - \boldsymbol{H}_h, \boldsymbol{H}_I - \boldsymbol{H}_h]_e, \tag{4.18}$$

and the estimate goes:

$$
\begin{aligned}
&\alpha_* \, \|\boldsymbol{H}_I - \boldsymbol{H}_h\|^2_{0,\Omega} \leq [\boldsymbol{H}_I - \boldsymbol{H}_h, \boldsymbol{H}_I - \boldsymbol{H}_h]_e \\
&= \text{(using (4.17))} \, [\boldsymbol{H}_I - \boldsymbol{H}_h, \mu \nabla q_h^*]_e \\
&= \text{(using the second of (4.13))} \, [\boldsymbol{H}_I, \mu \nabla q_h^*]_e \\
&= \text{(adding and subtracting } \Pi^0_{k-1}\boldsymbol{H}) \, [\boldsymbol{H}_I - \Pi^0_{k-1}\boldsymbol{H}, \mu \nabla q_h^*]_e + [\Pi^0_{k-1}\boldsymbol{H}, \mu \nabla q_h^*]_e \\
&= \text{(using (4.11))} \, [\boldsymbol{H}_I - \Pi^0_{k-1}\boldsymbol{H}, \mu \nabla q_h^*]_e + (\Pi^0_{k-1}\boldsymbol{H}, \mu \nabla q_h^*)_{0,\Omega} \\
&= \text{(adding and subtracting } \boldsymbol{H}) \, [\boldsymbol{H}_I - \Pi^0_{k-1}\boldsymbol{H}, \mu \nabla q_h^*]_e + (\Pi^0_{k-1}\boldsymbol{H} - \boldsymbol{H}, \mu \nabla q_h^*)_{0,\Omega} + (\boldsymbol{H}, \mu \nabla q_h^*)_{0,\Omega} \\
&= \text{(from the second of (2.14))} \, [\boldsymbol{H}_I - \Pi^0_{k-1}\boldsymbol{H}, \mu \nabla q_h^*]_e + (\Pi^0_{k-1}\boldsymbol{H} - \boldsymbol{H}, \mu \nabla q_h^*)_{0,\Omega} \\
&\leq \text{(using Cauchy–Schwarz and (4.9))} \left(\alpha^* \, \|\boldsymbol{H}_I - \Pi^0_{k-1}\boldsymbol{H}\|_{0,\Omega} + \|\Pi^0_{k-1}\boldsymbol{H} - \boldsymbol{H}\|_{0,\Omega}\right) \|\mu \nabla q_h^*\|_{0,\Omega} \\
&\leq \text{(from (4.17))} \left(\alpha^* \, \|\boldsymbol{H}_I - \Pi^0_{k-1}\boldsymbol{H}\|_{0,\Omega} + \|\Pi^0_{k-1}\boldsymbol{H} - \boldsymbol{H}\|_{0,\Omega}\right) \|\boldsymbol{H}_I - \boldsymbol{H}_h\|_{0,\Omega}
\end{aligned}
$$

that, using also (4.12), implies immediately

$$
\begin{aligned}
\|\boldsymbol{H}_I - \boldsymbol{H}_h\|_{0,\Omega} &\leq \frac{\alpha^*}{\alpha_*}(\|\boldsymbol{H}_I - \Pi^0_{k-1}\boldsymbol{H}\|_{0,\Omega} + \|\Pi^0_{k-1}\boldsymbol{H} - \boldsymbol{H}\|_{0,\Omega}) \\
&\leq \frac{2\alpha^*}{\alpha_*}(\|\boldsymbol{H} - \boldsymbol{H}_I\|_{0,\Omega} + \|\Pi^0_{k-1}\boldsymbol{H} - \boldsymbol{H}\|_{0,\Omega}).
\end{aligned}
$$

We can summarize the result in the following theorem.

Theorem 4.3. *Problem (4.13) has a unique solution and the following estimate holds:*

$$
\|\boldsymbol{H} - \boldsymbol{H}_h\|_{0,\Omega} \leq C \left(\|\boldsymbol{H} - \boldsymbol{H}_I\|_{0,\Omega} + \|\boldsymbol{H} - \Pi^0_{k-1}\boldsymbol{H}\|_{0,\Omega}\right), \tag{4.19}
$$

with C a constant independent of the mesh size. Moreover, thanks to (4.15) we also have

$$
\|rot(\boldsymbol{H} - \boldsymbol{H}_h)\|_{0,\Omega} = \|j - \Pi^0_{k_r} j\|_{0,\Omega}, \tag{4.20}
$$

so that

$$
\|\boldsymbol{H} - \boldsymbol{H}_h\|_{H(rot;\Omega)} \leq C \left(\|\boldsymbol{H} - \boldsymbol{H}_I\|_{0,\Omega} + \|\boldsymbol{H} - \Pi^0_{k-1}\boldsymbol{H}\|_{0,\Omega} + \|j - \Pi^0_{k_r} j\|_{0,\Omega}\right). \tag{4.21}
$$

The above result can be combined with standard polynomial approximation estimates on polygons in order to estimate the terms involving the L^2 projection on polynomials. Moreover, approximation estimates for the VEM interpolant H_I can be derived by a simple modification of the arguments in [55]. We therefore obtain, provided that $\boldsymbol{H}$ and j are sufficiently regular,

$$
\|\boldsymbol{H} - \boldsymbol{H}_h\|_{0,\Omega} \leq C h^s |\boldsymbol{H}|_{s,\Omega} \, , \qquad \|\text{rot}\,(\boldsymbol{H} - \boldsymbol{H}_h)\|_{0,\Omega} \leq C h^r |j|_{r,\Omega}, \tag{4.22}
$$

with $0 \leq s \leq k$ and $0 \leq r \leq k_r + 1$.

Remark 5. It should be pointed out that the proofs of both Proposition 4.2 and Theorem 4.3 rely heavily on (4.3), and on the chain (4.7)–(4.15)–(4.16) ending with (4.17) (which also needs (4.3)). The whole procedure is simple and neat, and follows classical arguments. However, it should be clear that, in particular, without (4.3) the whole construction would collapse and the proofs would become much more complicated. □

5. Serendipity spaces

Following a denomination started with $\mathbb{Q}_k$ Finite Element approximations on quadrilaterals, and then made popular in several other contexts, the Serendipity variants can be roughly described as *a reduction of the degrees of freedom operated without jeopardizing the expected accuracy*. In our context this implies, to start with, that we are going to keep all the boundary degrees of freedom in order to guarantee *conformity* (H^1 for nodal VEMs, and $H(\text{rot})$ for edge VEMs), keeping the existence of a *local basis*. Then, to the boundary d.o.f. we add all the internal d.o.f. that are necessary to ensure that the local VEM space contains, for nodal VEMs, all polynomials of the chosen degree (here: k), and for edge VEMs, all vector-valued polynomials of the chosen degree (here $(\mathbb{P}_{k-1})^2$), or, possibly, even some

bigger space if we have in mind the accuracy of $N1$-like spaces (see (2.12)), for instance if we need to be as accurate in $H(\mathrm{rot})$ as we are in $(L^2)^2$.

In what follows, therefore, we go back to the nodal and edge spaces defined in (3.1) and (3.10) and we want to define their Serendipity versions, in order to reduce the internal degrees of freedom as much as possible. For the sake of simplicity, setting

$$\eta = \text{ minimum number of straight lines necessary to cover the boundary,}$$

we assume first that, on each polygon E, the degree k is smaller than η. This means to assume that the geometry of E is such that every polynomial of degree k vanishing on all ∂E is identically zero: in other words, we are *assuming* that

$$\mathbb{P}_k(E) \textit{ does not contain bubbles}. \tag{5.1}$$

At the end of the Section we will also give indications for higher values of k (for simplicity on convex polygons).

5.1. Local serendipity nodal spaces

For the **nodal** Virtual elements we define a projection $\Pi^n_S : V^n_k(E) \to \mathbb{P}_k(E)$ by

$$\begin{cases} \displaystyle\int_{\partial E} \partial_t(q - \Pi^n_S q)\partial_t p \,\mathrm{d}s = 0 \quad \forall p \in \mathbb{P}_k(E), \\ \displaystyle\int_{\partial E} (\boldsymbol{x}_{\mathrm{E}} \cdot \boldsymbol{n})(q - \Pi^n_S q)\,\mathrm{d}s = 0, \end{cases} \tag{5.2}$$

where again $\boldsymbol{x}_{\mathrm{E}} = \boldsymbol{x} - \mathbf{b}_{\mathrm{E}}$, with $\mathbf{b}_{\mathrm{E}} =$ barycenter of E, and ∂_t denotes the derivative along the boundary.

Proposition 5.1. *The operator Π^n_S is well defined.*

Proof. Indeed, the number of conditions in (5.2) being equal to the dimension of $\mathbb{P}_k$, we have to check that for $\Pi^n_S q \in \mathbb{P}_k(E)$ we have

$$\left\{ \int_{\partial E} \partial_t \Pi^n_S q \;\partial_t p \,\mathrm{d}s = 0 \;\; \forall p \in \mathbb{P}_k(E) \text{ and } \int_{\partial E} (\boldsymbol{x}_{\mathrm{E}} \cdot \boldsymbol{n}) \Pi^n_S q \,\mathrm{d}s = 0 \right\} \implies \Pi^n_S q \equiv 0.$$

The first condition implies $\Pi^n_S q$ constant on each edge, and hence (recalling (5.1)) $\Pi^n_S q = c$ in E. The second condition gives $c = 0$, observing that

$$\int_{\partial E} (\boldsymbol{x}_{\mathrm{E}} \cdot \boldsymbol{n})\,\mathrm{d}s = \int_E \mathrm{div}\, \boldsymbol{x}_{\mathrm{E}} \,\mathrm{d}E = 2|E|. \tag{5.3}$$

We point out that for $q \in V^n_k(E)$ we can compute $\Pi^n_S q$ using only the boundary degrees of freedom (3.2) and (3.3). □

Then we introduce, for $k \geq 2$, **the Serendipity nodal space** as:

$$SV^n_k(E) = \left\{ q \in V^n_k(E) \,:\, \int_E (\nabla q - \nabla \Pi^n_S q) \cdot \boldsymbol{x}_{\mathrm{E}}\, p_{k_d} \,\mathrm{d}E = 0 \,\forall p_{k_d} \in \mathbb{P}_{k_d} \right\}. \tag{5.4}$$

Using that $\Pi^n_S q$ depends only on the boundary values of q, one can check that a set of degrees of freedom for the space $SV^n_k(E)$ is given by the nodal values at the vertices of E and the moments of order $k-2$ on the edges, i.e., (3.2)–(3.3). Clearly, we have

$$\mathbb{P}_k(E) \subseteq SV^n_k(E) \subseteq V^n_k(E).$$

Remark 6. We also note that for $q \in SV^n_k$ one can use its degrees of freedom (that, as we saw, are just (3.2) and (3.3)) to compute $\Pi^n_S q$ through (5.2), and then compute its moments (3.4) (since, following (5.4), the moments (3.4) of q and of $\Pi^n_S q$ are the same). In other words, for a $q \in SV^n_k$, the knowledge of the degrees of freedom (3.2) and (3.3) allows the computation of the degrees of freedom (3.4) (and then, in particular, as shown in Proposition 3.2, the computation of the L^2-projection of ∇q onto $[\mathbb{P}_{k-1}(E)]^2$). □

Remark 7. We also point out that, when dealing with SV_k^n on the computer, one uses only the degrees of freedom (3.2) and (3.3), and they **do not** depend on the value of k_d. This means that for $q \in SV_k^n$ one can always think that, say, $k_d = k$ and use the moments of $\Pi_S^n q$ as being the moments of q up to the order k. Note also that to use moments of an order higher than k would be correct but useless: $\Pi_S^n q$ is, itself, in $\mathbb{P}_k$, and its projection on a bigger space will not change it. □

Remark 8. Note that the procedure for the construction of Serendipity Virtual Elements is **quite different** from the one that is normally used for Finite Elements. There (on FEM), the basic procedure is to present the reduced (Serendipity) space as the span of: {$\mathbb{P}_k$ plus some additional monomials, or some explicitly and suitably chosen polynomials of degree higher than k}. Then the degrees of freedom for the Serendipity space can be chosen in an almost arbitrary way, taking into account the practical convenience. For Virtual Elements, on the contrary, the construction of the Serendipity space $SV_k^n(E)$ is based on the choice of the projection operator Π_S^n in (5.2), that, in turn, uses a subset of the degrees of freedom used for the starting space $V_k^n(E)$, and requires also the choice of some sort of inner product. For instance here, in (5.2), we used a sort of $H^1(\partial E)$ inner product, while in [39] we used instead an Euclidean inner product among the chosen degrees of freedom. Taking one choice or the other for the degrees of freedom **and** for the scalar products will clearly change the definition of the projection operator Π_S^n, and this will **change the space** $SV_k^n(E)$. Note that the change will not (essentially, in all cases) be restricted to the formal way of defining it: it will actually be a true change of the elements that belong to the space (apart, obviously, from the elements of $\mathbb{P}_k$, that will remain untouchable). In general, therefore, we might expect that a change in the original degrees of freedom in $V_k^n(E)$ or a change in the inner product(s) used to define the projection operator Π_S^n will end up in a **different Serendipity space** having **different properties.** □

5.2. Local serendipity edge spaces

For the **edge** Virtual elements, instead, we should, in principle, distinguish two cases: whether we want to preserve just the space $N2_{k-1} \equiv [\mathbb{P}_{k-1}(E)]^2$ or the (bigger) space $N1_{k-1} \equiv \{\boldsymbol{v} \in [\mathbb{P}_{k-1}(E)]^2 \text{ with rot } \boldsymbol{v} \in \mathbb{P}_{k-1}(E)\}$ (see (2.12) and (2.13)). The difference between the two cases is in the choice of k_r: $k_r = k-2$ and $k_r = k-1$, respectively. We will treat, as far as possible, the two cases together. For this we introduce the space

$$S_{k-1}^e := \mathbf{grad}\, \mathbb{P}_k \oplus \boldsymbol{x}^{\perp} \mathbb{P}_{k_r}, \tag{5.5}$$

that corresponds to $N2$ when $k_r = k-2$, and to $N1$ when $k_r = k-1$ (see again (2.12) and (2.13)). We point out that, in both cases

$$\text{dimension}(S_{k-1}^e) = \pi_{k,2} - 1 + \pi_{k_r,2}. \tag{5.6}$$

We can now define a projection $\Pi_S^e : V_{k-1}^e(E) \to S_{k-1}^e$ as follows:

$$\int_{\partial E} [(\boldsymbol{v} - \Pi_S^e \boldsymbol{v}) \cdot \boldsymbol{t}][\nabla p \cdot \boldsymbol{t}]\, \mathrm{d}s = 0 \quad \forall p \in \mathbb{P}_k(E), \tag{5.7}$$

$$\int_{\partial E} (\boldsymbol{v} - \Pi_S^e \boldsymbol{v}) \cdot \boldsymbol{t}\, \mathrm{d}s = 0, \tag{5.8}$$

$$\int_E \text{rot}\, (\boldsymbol{v} - \Pi_S^e \boldsymbol{v}) p_{k_r}^0\, \mathrm{d}E = 0 \quad \forall p_{k_r}^0 \in \mathbb{P}_{k_r}^0(E). \tag{5.9}$$

Proposition 5.2. *The operator Π_S^e is well defined.*

Proof. Indeed, the number of conditions in (5.7)–(5.9) being equal to the dimension of S_{k-1}^e, we need to check that for $\Pi_S^e \boldsymbol{v} \in S_{k-1}^e$ the conditions

$$\int_{\partial E} [\Pi_S^e \boldsymbol{v} \cdot \boldsymbol{t}][\nabla p \cdot \boldsymbol{t}]\, \mathrm{d}s = 0 \quad \forall p \in \mathbb{P}_k(E), \tag{5.10}$$

$$\int_{\partial E} \Pi_S^e \boldsymbol{v} \cdot \boldsymbol{t}\, \mathrm{d}s = 0, \tag{5.11}$$

$$\int_E \text{rot}\, (\Pi_S^e \boldsymbol{v}) p_{k_r}^0\, \mathrm{d}E = 0 \quad \forall p_{k_r}^0 \in \mathbb{P}_{k_r}(E), \tag{5.12}$$

imply $\Pi^e_S \boldsymbol{v} \equiv 0$. It is easy to see that (5.11) and (5.12), together, imply rot $(\Pi^e_S \boldsymbol{v}) = 0$, so that $\Pi^e_S \boldsymbol{v} = \nabla p_k$ for some $p_k \in \mathbb{P}_k(E)$. Then (5.10) gives $\Pi^e_S \boldsymbol{v} \cdot \boldsymbol{t} = 0$ and using (5.1) we deduce $\Pi^e_S \boldsymbol{v} = 0$. □

We can now define **the Serendipity edge space** as:

$$SV^e_{k-1}(E) = \left\{ \boldsymbol{v} \in V^e_{k-1}(E) \ : \ \int_E (\boldsymbol{v} - \Pi^e_S \boldsymbol{v}) \cdot \boldsymbol{x}_E \, p_{k_d} \, \mathrm{d}E = 0 \quad \forall p_{k_d} \in \mathbb{P}_{k_d} \right\}. \tag{5.13}$$

Again by a standard procedure one can check that a set of degrees of freedom for the space $SV^e_{k-1}(E)$ is made by the edge moments (3.11)), and by the rot -moments (3.13). Clearly, we have

$$S^e_{k-1} \subset SV^e_{k-1}(E) \subset V^e_{k-1}(E). \tag{5.14}$$

Remark 9. Mimicking Remarks 6 and 7 we point out that for elements $\boldsymbol{v} \in SV^e_{k-1}(E)$ we can use the d.o.f.s (3.11) and (3.13), compute $\Pi_S \boldsymbol{v}$ using (5.7)–(5.9), and then use $\Pi_S \boldsymbol{v}$ to get the values of the d.o.f.s (3.12). Then, in particular, we can compute the projection Π^0_{k-1} on $(\mathbb{P}_{k-1})^2$, and so on. □

Remark 10. Similarly to what we pointed out in Remark 8 for nodal Serendipity Virtual Element spaces, we have here that the edge Serendipity spaces $SV^e_{k-1}(E)$ defined in (5.13) depend on the projection operator Π^e_S, that in turn depends on the degrees of freedom that are chosen, and on the type of scalar product used to define it. Here too, different degrees of freedom and different scalar products will produce different Serendipity spaces with different properties. □

In order to proceed to the Serendipity discretization of the magneto-static problem (1.1) and to analyze its convergence properties, a crucial step well be the proof of the Serendipity version of the fundamental property (4.3). This needs first the following Lemma.

Lemma 5.3.

$$\nabla \, \Pi^n_S q = \Pi^e_S \, \nabla q \qquad \forall q \in SV^n_k(E). \tag{5.15}$$

Proof. We have to prove that conditions (5.7)–(5.9) (for $\boldsymbol{v} \equiv \nabla q$) are satisfied when using $\nabla \, \Pi^n_S q$ in place of $\Pi^e_S \, \nabla q$. Using the first equation in (5.2) we have, for all $p \in \mathbb{P}_k(E)$,

$$\sum_{e \in \partial E} \int_e \Big[(\nabla q - \nabla \Pi^n_S q) \cdot \boldsymbol{t}_e \Big] \Big[\nabla p \cdot \boldsymbol{t}_e \Big] \, \mathrm{d}s \equiv \sum_{e \in \partial E} \int_e \partial_t (q - \Pi^n_S q) \partial_t p \, \mathrm{d}s = 0,$$

so that (5.7) holds true. Moreover, as both q and $\Pi^n_S q$ are in $C^0(\partial E)$, we obviously have

$$\sum_{e \in \partial E} \int_e (\nabla q - \nabla \Pi^n_S q) \cdot \boldsymbol{t}_e = \int_{\partial E} \partial_t (q - \Pi^n_S q) \, \mathrm{d}s = 0,$$

that gives (5.8). Finally it is obvious that

$$\int_E \text{rot} \, (\nabla (q - \Pi^n_S q)) p^0_{k_r} \, \mathrm{d}E = 0 \quad \forall p^0_{k_r} \in \mathbb{P}^0_{k_r}(E),$$

giving (5.9) and ending the proof. □

Remark 11. Identity (5.15) is particularly useful from the computational point of view. Indeed, looking at the definition (5.4) of the serendipity nodal space, we see that it allows us to build *only* the serendipity projection operator for the edge space, and use it for constructing $SV^n_k(E)$. □

5.3. The coupling of serendipity nodal and edge spaces

Now we want to prove the Serendipity version of (4.3).

Proposition 5.4. *With the above definitions we have*

$$\nabla\, SV_k^n(E) = \Big\{ \boldsymbol{v} \in SV_{k-1}^e(E) \ :\ \mathit{rot}\, \boldsymbol{v} = 0 \Big\}. \tag{5.16}$$

Proof. Clearly for each $q \in SV_k^n(E)$ the function $\boldsymbol{v} = \nabla q$ verifies $\boldsymbol{v} \cdot \boldsymbol{t}_{|e} \in \mathbb{P}_{k-1}(e)$ on each edge e, $\operatorname{div} \boldsymbol{v} = \Delta q \in \mathbb{P}_{k_d}(E)$, and $\operatorname{rot} \nabla q = 0$. Moreover the condition

$$\int_E (\nabla q - \Pi_S^e \nabla q) \cdot \boldsymbol{x}_E\, p_{k_d}\, \mathrm{d}E = 0 \quad \forall p_{k_d} \in \mathbb{P}_{k_d} \tag{5.17}$$

is automatically verified using (5.15) and the definition of the nodal Serendipity space (5.4). Conversely, for a $\boldsymbol{v} \in SV_{k-1}^e(E)$ with $\operatorname{rot} \boldsymbol{v} = 0$ we clearly have, from (4.3), that $\boldsymbol{v} = \nabla q$ for some $q \in V_k^n$, and using first (5.15), then $\nabla q = \boldsymbol{v}$, and finally that $\boldsymbol{v} \in SV_{k-1}^e(E)$, we have for all $p_{k_d} \in \mathbb{P}_{k_d}$:

$$\int_E (\nabla q - \nabla \Pi_S^n q) \cdot \boldsymbol{x}_E\, p_{k_d}\, \mathrm{d}E = \int_E (\nabla q - \Pi_S^e \nabla q) \cdot \boldsymbol{x}_E\, p_{k_d}\, \mathrm{d}E = \int_E (\boldsymbol{v} - \Pi_S^e \boldsymbol{v}) \cdot \boldsymbol{x}_E\, p_{k_d}\, \mathrm{d}E = 0 \tag{5.18}$$

implying that q is actually in SV_k^n (see (5.4)). □

Remark 12. It is easy to see that property (5.15) is essential in (5.16). We can see that the choices of the degrees of freedom in the original (non Serendipity) nodal and edge Virtual Element Spaces, together with the choices of the projection operators, are essential (and, in our opinion, non trivial) in order to have the property (5.16), which is the Serendipity counterpart of (4.3), that, in turn, was the key to the convergence proof of Theorem 4.3. □

Remark 13. We point out that the definition (5.7)–(5.9) of the projection operator Π_S^e implies, in particular, that $\operatorname{rot} \boldsymbol{v}$ and $\operatorname{rot} \Pi_S^e \boldsymbol{v}$ are equal. Then it is immediate to see that, similarly to (4.5), we also have

$$\operatorname{rot} SV_{k-1}^e \equiv V_{k_r}^E. \quad \square \tag{5.19}$$

The global spaces are the obvious extension of the local ones, and so are the global degrees of freedom. Denoting the global spaces by $SV_{k-1}^e(\Omega)$ and $SV_k^n(\Omega)$, the discrete problem with the Serendipity spaces is

$$\begin{cases} \text{find } \boldsymbol{H}_h \in SV_{k-1}^e(\Omega) \text{ and } p_h \in SV_k^n(\Omega) \text{ such that:} \\ \displaystyle\int_\Omega \operatorname{rot} \boldsymbol{H}_h \operatorname{rot} \boldsymbol{v}\, \mathrm{d}\Omega + [\nabla p_h, \mu \boldsymbol{v}]_e = \int_\Omega j \operatorname{rot} \boldsymbol{v}\, \mathrm{d}\Omega \quad \forall \boldsymbol{v} \in SV_{k-1}^e(\Omega), \\ [\nabla q, \mu \boldsymbol{H}_h]_e = 0 \quad \forall q \in SV_k^n(\Omega). \end{cases} \tag{5.20}$$

Thanks to the inclusion (5.14), the scalar products (3.14) and (4.8) can still be used, and the crucial equality (5.16) allows us to prove uniqueness of the solution of (5.20), together with the error estimates (4.19) and (4.21) exactly as we did in the previous section.

6. The case of $k \geq \eta$

It is relatively simple to extend the previous discussion on Serendipity nodal and edge VEMs to the case of a k that is greater or equal to the number η of edges necessary to cover ∂E. For simplicity we will just tackle the case of convex polygons. In what follows we will set

$$\beta := k - \eta.$$

As we shall see in a while, a crucial role in the Serendipity VEMs with a higher k is played by the space of bubbles

$$B_k = \{q \in \mathbb{P}_k(E) \text{ such that } q \equiv 0 \text{ on } \partial E\}, \tag{6.1}$$

that clearly can be written as

$$B_k = b_\eta \mathbb{P}_\beta, \tag{6.2}$$

where b_η is **the** polynomial of degree η that vanishes identically on ∂E and, say, is equal to 1 at the barycenter $\mathbf{b}_E$ of E. Note that, for a convex polygon E, we easily have $b_\eta > 0$ at all points internal to E.

In this case, the Serendipity projection Π^n_S, in order to be well defined, needs, in addition to (5.2), the conditions

$$\int_E (\nabla(q - \Pi^n_S q)) \cdot \boldsymbol{x}_{\mathrm{E}} p_\beta \, \mathrm{d}E = 0 \quad \forall p_\beta \in \mathbb{P}_\beta. \tag{6.3}$$

To check that adding (6.3) to (5.2) the operator Π^n_S is well defined, we proceed as we did in Proposition 5.1. Assuming that we have

$$\int_{\partial E} \partial_t \Pi^n_S q \;\; \partial_t p \, \mathrm{d}s = 0 \;\; \forall p \in \mathbb{P}_k(E), \tag{6.4}$$

$$\int_{\partial E} (\boldsymbol{x}_{\mathrm{E}} \cdot \boldsymbol{n}) \Pi^n_S q \, \mathrm{d}s = 0, \tag{6.5}$$

$$\int_E \nabla \Pi^n_S q \cdot \boldsymbol{x}_{\mathrm{E}} p_\beta \, \mathrm{d}E = 0 \quad \forall q_\beta \in \mathbb{P}_\beta, \tag{6.6}$$

from (6.4) and (6.5) we immediately deduce, as before, that $\Pi^n_S q = 0$ on ∂E. Hence, $\Pi^n_S q \in B_k$, so that (6.2) gives $\Pi^n_S q = b_\eta p^*_\beta$ for some $p^*_\beta \in \mathbb{P}_\beta$. Integrating (6.6) by parts, and using (2.10) we obtain

$$\int_E (\Pi^n_S q) p_\beta \, \mathrm{d}E = 0 \quad \forall p_\beta \in \mathbb{P}_\beta, \tag{6.7}$$

that used with $\Pi^n_S q = b_\eta p^*_\beta$ and $p_\beta = p^*_\beta$ gives

$$\int_E b_\beta (p^*_\beta)^2 \, \mathrm{d}E = 0$$

which implies $\Pi^n_S q \equiv 0$. Having defined the projection $q \to \Pi^n_S q$ we can now define the Serendipity space $SV^n_k(E)$ as

$$SV^n_k(E) = \left\{ q \in V^n_k(E) \; : \; \int_E (\nabla q - \nabla \Pi^n_S q) \cdot \boldsymbol{x}_{\mathrm{E}} \, p \, \mathrm{d}E = 0 \, \forall p \in \mathbb{P}_{\beta/k_d} \right\}, \tag{6.8}$$

where $\mathbb{P}_{\beta/k_d}$ is the space spanned by the homogeneous polynomials of degree s with $\beta < s \leq k_d$.

Remark 14. From the above discussion, we see that the degrees of freedom (3.2), (3.3) and, whenever $\beta \geq 0$

$$\int_E (\nabla q \cdot \boldsymbol{x}_{\mathrm{E}}) p_\beta \, \mathrm{d}E \quad \forall p_\beta \in \mathbb{P}_\beta, \tag{6.9}$$

will be a unisolvent set of degrees of freedom in $SV^n_k(E)$, and that, arguing as in Remarks 6 and 7, they will allow the computation of the L^2-orthogonal projection on $\mathbb{P}_k$ as well as the $(L^2)^2$-orthogonal projection of the gradients on $(\mathbb{P}_{k-1})^2$. □

The very same logic applies to the Serendipity edge case for $k \geq \eta$, where now the definition of the projection $\Pi^e_S \boldsymbol{v}$ would require the additional conditions

$$\int_E (\boldsymbol{v} - \Pi^e_S \boldsymbol{v}) \cdot \boldsymbol{x}_{\mathrm{E}} \, p_\beta \, \mathrm{d}E \quad \forall p_\beta \in \mathbb{P}_\beta(E). \tag{6.10}$$

The Serendipity edge space will then be

$$SV^e_{k-1}(E) = \left\{ \boldsymbol{v} \in V^e_{k-1}(E) \; : \; \int_E (\boldsymbol{v} - \Pi^e_S \boldsymbol{v}) \cdot \boldsymbol{x}_{\mathrm{E}} \, p \, \mathrm{d}E = 0 \, \forall p \in \mathbb{P}_{\beta/k_d} \right\}. \tag{6.11}$$

Remark 15. In the same spirit of that of Remark 14 we see that the degrees of freedom (3.11), (3.13), supplemented (for $\beta \geq 0$) with

$$\int_E (\boldsymbol{v} \cdot \boldsymbol{x}_{\mathrm{E}}) p_\beta \, \mathrm{d}E \quad \forall p_\beta \in \mathbb{P}_\beta, \tag{6.12}$$

will be a unisolvent set of degrees of freedom in $SV^e_{k-1}(E)$, and that they will allow the computation of the $(L^2)^2$-orthogonal projection on $(\mathbb{P}_{k-1})^2$. □

Then we can just proceed following step by step (with the minor obvious adaptations) what we did in the previous Section.

The case of *non-convex* E can also be reasonably easily dealt with (essentially, using b_k in place of p_k in (6.3) and in (6.10)). We refer to [39] and [40] for the necessary background.

7. Numerical results

In this section we numerically validate the proposed VEM theory for 2D magnetostatic problems. We set $k_d = k-2$ and $k_r = k-1$ in the definition of the virtual nodal and edge spaces. We will analyze different aspects of the proposed method. For this, we set $\mu = 1$, $\Omega = [0,\ 1]^2$ and take as exact solution of (1.1)

$$\boldsymbol{H}(x,\ y) := \begin{pmatrix} -\pi\ \cos(\pi x)\ \sin(\pi y) \\ \pi\ \sin(\pi x)\ \cos(\pi y) \end{pmatrix}.$$

It is easy to verify that $\boldsymbol{H}\cdot\boldsymbol{t} = 0$ on $\partial\Omega$ and $j := \mathrm{rot}\,\boldsymbol{H}$ has zero mean value.

We discretize the unit square $\Omega = [0,\ 1]^2$ in four different ways, see Fig. 1:

- `quadN`: structured mesh composed by `N` squares;
- `voroN`: mesh composed by `N` Voronoi cells;
- `rhexN`: mesh composed by `N` regular hexagons.
- `dhexN`: mesh composed by `N` distorted hexagons.

The mesh-size h is defined as

$$h := \frac{1}{N}\sum_{E\in\mathcal{T}_h} h_E\,, \tag{7.1}$$

where N is the number of mesh elements and h_E is the diameter of the element E. Then, for each type of mesh, we will consider a sequence of four meshes with decreasing mesh size h to make the error convergence analysis. More specifically, for `quadN` and `voroN` we have `N` $= 100, 400, 1600$ and 6400, while for `rhexN` and `dhexN` we have `N` $= 94, 389, 1415$ and 5711, in order to have essentially the same h for all mesh types. We then apply the serendipity approach described in Sections 5 and 6, choosing the space $N1_{k-1}$ as edge space (see Eq. (2.12)). Before showing the numerical results, we underline that the serendipity version of Section 6 is essential for elements E with $k \geq \eta_E$, since the recipe of Section 5 fails in this case.

In Fig. 2 we provide the convergence graphs with the serendipity approach and the standard one. For completeness we also report the case $k = 1$, where there are no internal dofs, and hence no serendipity is needed. Fig. 2 shows the convergence rate of the L^2 error, computed as

$$\frac{\|\boldsymbol{H} - \Pi^0_{k-1}\boldsymbol{H}_h\|_{0,\,\Omega}}{\|\boldsymbol{H}\|_{0,\,\Omega}}.$$

The trend of this error is coherent with the theory for all the meshes taken into account. What is also important, in our opinion, is to check that using the Serendipity version of nodal and edge VEM spaces we have the same accuracy and almost exactly the same results that we have when using the full VEM spaces.

The exact solution p_h of the discretized problem is identically zero. Clearly, the roundoff errors generate, out of the computer, a p_h that is *almost* identically zero. In some sense we could take the values of the *computed* p_h as a measure (or, better, a rough indicator) of the conditioning of the final linear system. In particular, we compared the values of p_h for the original discretization (4.13) with the values of p_h for the Serendipity version (5.20) to have some information on the conditioning of the linear system. In Table 3 we provide the maximum absolute value of the dofs of p_h, i.e., we compute $\max|dof\ (p_h)|$, where $dof\ (p_h)$ denotes the array of the dofs of the function p_h in the space V_k^n. In this table we consider only the nested meshes `dhexN`, similar results are obtained for the other mesh types. All these values are sufficiently close to the machine precision and they grow with the degree k.

We note that, since we are solving a lower dimensional linear system, the dof values of the scalar function p_h computed with the serendipity approach are closer to the machine precision than those obtained with the standard procedure, see Table 3.

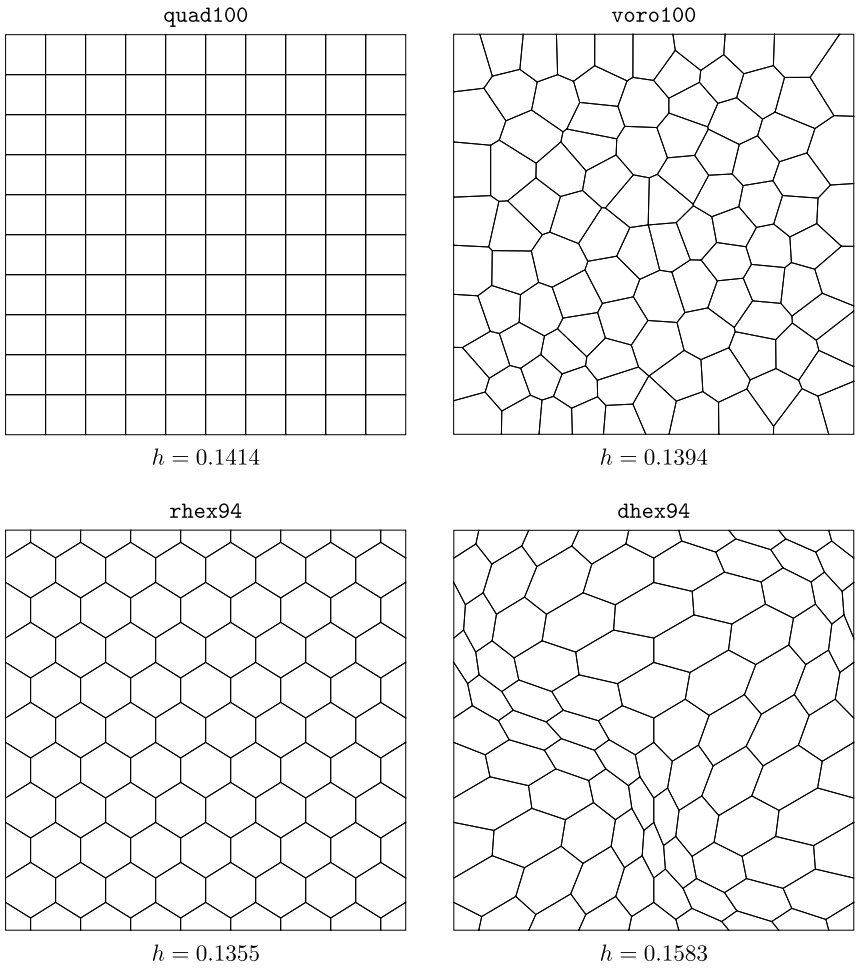

Fig. 1. Different discretizations of the unit square $[0,\ 1]^2$.

Table 3
Comparison between the values of $\max|dof\ (p_h)|$ obtained via a standard and a serendipity approach. We consider the set of nested mesh `dhexN` and similar results are obtained for the other set of meshes.

k	Approach	`dhex94`	`dhex389`	`dhex1415`	`dhex5711`
1	Standard	1.1875e−14	3.4438e−14	2.1061e−13	7.1641e−13
2	Standard	1.9811e−13	2.7685e−12	2.3027e−11	2.0194e−10
	Serendipity	1.2651e−14	4.5334e−14	1.3284e−13	1.6533e−12
3	Standard	2.8698e−11	3.4730e−10	1.8091e−09	8.5544e−08
	Serendipity	1.1454e−12	3.1212e−12	1.2349e−11	1.4966e−10
4	Standard	2.5490e−11	8.2772e−11	2.7047e−09	6.9675e−08
	Serendipity	2.2063e−12	8.3612e−12	5.1823e−11	3.5685e−10

To better understand the advantage of the serendipity approach in terms of reduction of the number of degrees of freedom, we compute the following quantity

$$\texttt{gain} := 100\,\frac{\#dof - \#dof_S}{\#dof}\%\,,$$

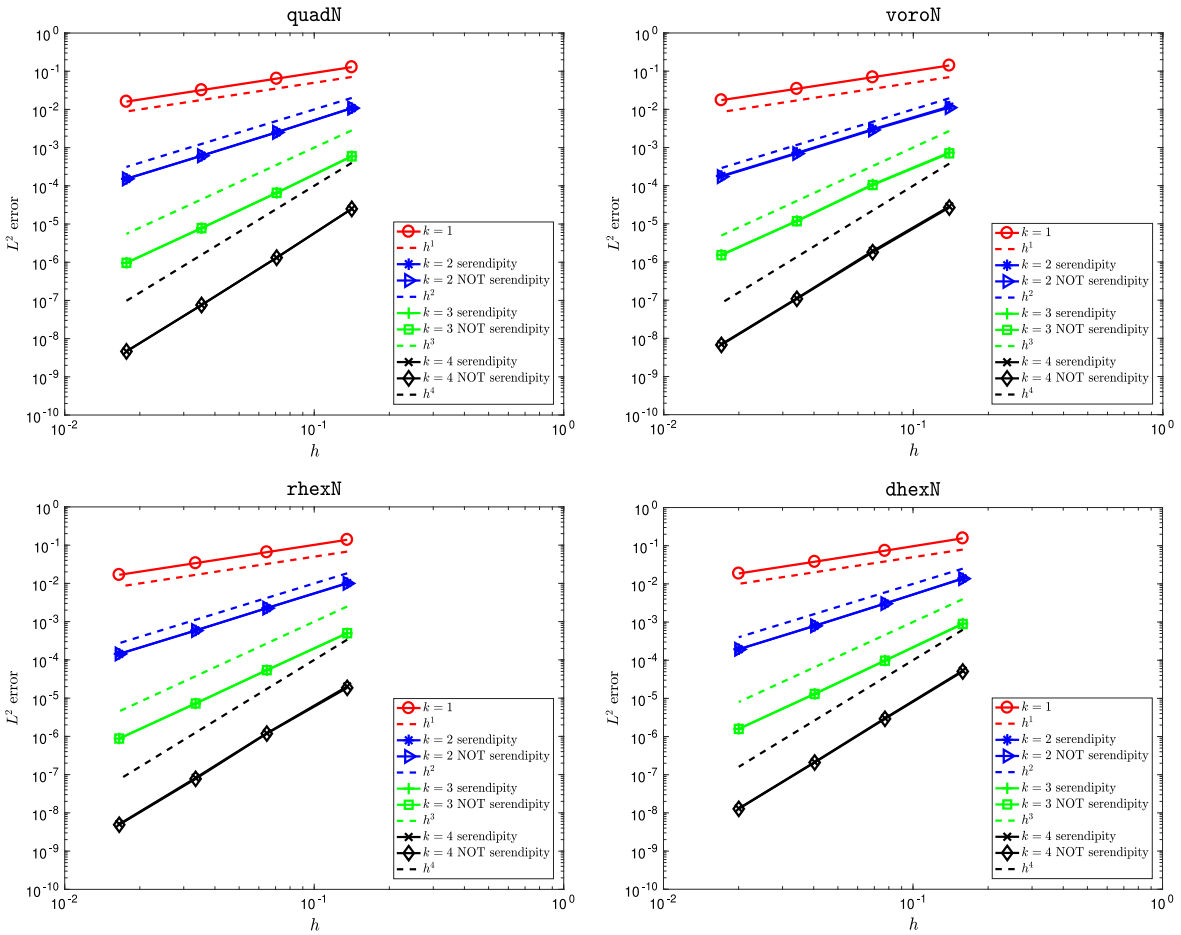

Fig. 2. Comparison of the L^2-error h-convergence rates for standard and serendipity approach varying the mesh types and the VEM degrees k.

Table 4
Example of gain on the number of degrees of freedom with the serendipity procedure.

k	quad1600	voro1600	rhex1415	dhex1415
2	17.85%	13.33%	13.33%	13.33%
3	26.90%	21.42%	21.42%	21.42%
4	27.47%	27.13%	27.13%	27.13%

where $\#dof$ and $\#dof_S$ are the number of degrees of freedom with the standard and the serendipity approach, respectively. In Table 4 we provide the value of gain only for one example of each kind of mesh; similar results are obtained for the other meshes. The gain in terms of degrees of freedom is remarkable and it increases with the degree k.

7.1. Numerical experiment with singular solution

In this subsection we solve problem (1.1) on a standard L-Shaped domain $\Omega \subset [-1,\ 1]^2$, we set again $\mu = 1$, and we choose the right hand side f and the boundary conditions in such a way that the exact solution is

$$\boldsymbol{H}(x,\ y) := \nabla\zeta(x,\ y) + \begin{pmatrix} -y \\ x \end{pmatrix},$$

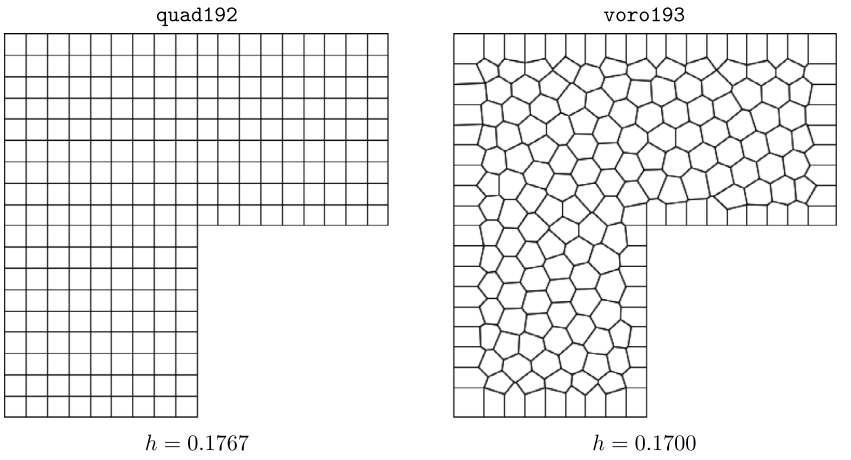

Fig. 3. Different discretizations of the L-shape domain.

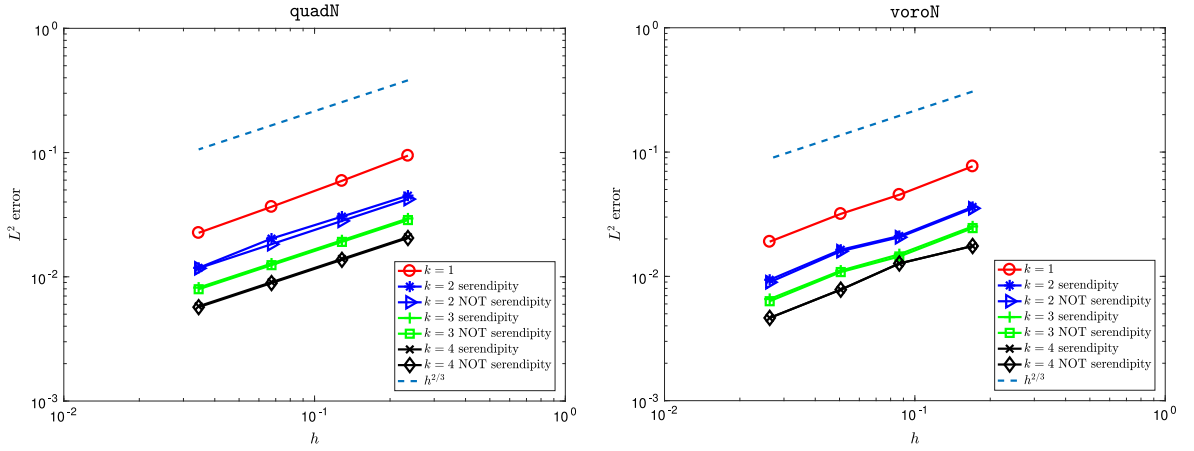

Fig. 4. Comparison of the L^2-error h-convergence rates for standard and serendipity approach varying the mesh types and the VEM degrees k.

where $\nabla\zeta(x,\ y)$ is the gradient of the function ζ defined via the standard polar coordinate system θ, ρ

$$\zeta(\theta,\ \rho) \coloneqq \rho^{2/3}\ \sin\left(\frac{2}{3}\,\theta\right).$$

We observe that the function ζ is harmonic and thus the vector field $\boldsymbol{H}$ is divergence free, which is in agreement with (1.1). Moreover, since the function $\zeta \in H^{1+\frac{2}{3}-\epsilon}(\Omega),\ \forall\epsilon > 0$, the vector field $\boldsymbol{H} \in H^{\frac{2}{3}-\epsilon}(\Omega)$. We then expect a convergence rate of about $h^{2/3}$ for each VEM approximation degree k, see Eq. (4.22).

As before we consider a sequence of nested meshes of equal squares, `quadN`, and of well-shaped Voronoi cells, `voroN`, where `N` is the number of elements, see Fig. 3. More specifically, we take `N` $= 100, 400, 1600$ and 6400 for the mesh of squares, and `N` $= 193, 699, 2050$ and 7225 for the Voronoi mesh. Also in this case we chose the edge space $N1_{k-1}$ in the serendipity approach.

In Fig. 4 we provide the convergence graphs with both the standard and the serendipity approach. The error behaves as expected: for each degree k the convergence rate is approximately $2/3$, and the accuracy improves when k grows, as expected (see, e.g., [17,18,47,48]). Moreover, the serendipity approach is indistinguishable from the corresponding standard one for all k. Finally, we do not report the results for the scalar variable p_h since it vanishes up to machine precision also in this case.

8. A glimpse to the 3D case

In this section we give a brief hint on the use of the machinery of the previous sections for the three-dimensional case (although this is actually beyond the scopes of the present paper). We limit ourselves to the definition of the local spaces, as the rest of the development is still work in progress.

8.1. The local VEM spaces in 3D

Let therefore P be a simply connected polyhedron, with the usual starshapedness assumptions on the polyhedron itself and on each of its faces f. For simplicity, we will assume that each face f of $\mathbb{P}$ is convex.

For an integer k, fixed (as we did in 2 dimensions) once and for all, for each face f we will use the spaces Serendipity $SV_k^n(f)$ and $SV_{k-1}^e(f)$ as defined in (5.4) and (5.13)–(3.10) (with $k_r = k-1$), respectively.

Remark 16. The name of the game, here, is to use the Serendipity VEM spaces only at the inter-element boundaries, without attempting to reduce the number of degrees of freedom (and to make the spaces slimmer) inside P. In other words, we label the d.o.f.s internal to P as "bound to disappear, out of static condensation". □

We then introduce the three-dimensional analogues of (5.4) and (5.13) that are

$$V_k^n(\mathrm{P}) := \Big\{ q : q_{|f} \in SV_k^n(f),\ \forall \text{ face } f \in \partial\mathrm{P},\ \Delta q \in \mathbb{P}_{k-2} \Big\}, \tag{8.1}$$

$$\begin{aligned} V_{k-1}^e(\mathrm{P}) := \quad \Big\{ \boldsymbol{v} : \boldsymbol{v}\cdot\boldsymbol{t} \text{ continuous on each edge } e \in \partial\mathrm{P}, \boldsymbol{v}_{|f} \in SV_{k-1}^e(f)\ \forall \text{ face } f \in \partial\mathrm{P}, \\ \operatorname{div}\boldsymbol{v} \in \mathbb{P}_{k-2}(\mathrm{P}),\ \mathbf{curl}\,(\mathbf{curl}\,\boldsymbol{v}) \in (\mathbb{P}_{k-2}(\mathrm{P}))^3 \Big\}. \end{aligned} \tag{8.2}$$

Actually, in 3 dimensions we would also need a Virtual Element Face space, that we define as

$$V_{k-1}^f(\mathrm{P}) := \Big\{ \boldsymbol{w} | \boldsymbol{w}\cdot\boldsymbol{n}_f \in \mathbb{P}_{k-1}(f)\ \forall \text{ face } f,\ \operatorname{div}\boldsymbol{w} \in \mathbb{P}_{k-1}(\mathrm{P}),\ \mathbf{curl}\,\boldsymbol{w} \in (\mathbb{P}_{k-2}(\mathrm{P}))^3 \Big\}. \tag{8.3}$$

Remark 17. We note that, in many applications, the number of internal degrees of freedom for the spaces (8.1), (8.2), and (8.3) will be more than necessary. However, as already pointed out in Remark 16, we will not make efforts to diminish them, as we assume that in practice we could eliminate them by static condensation. □

Remark 18. We also point out that for the Face three-dimensional space we **do not** need a Serendipity version on faces (as we do for nodal and edge elements) since the normal component (that is what we use on faces) is already a $\mathbb{P}_{k-1}$ polynomial and cannot be further reduced without jeopardizing the accuracy. □

We easily see that, with the above definitions, for every $q \in V_k^n(\mathrm{P})$, we have that the *tangential gradient*, applied *face by face*, belongs to $SV_{k-1}^e(f)$. Consequently, we also have, almost for free, the crucial property

$$\nabla\Big(V_k^n(\mathrm{P})\Big) \equiv \Big\{ \boldsymbol{v} \in V_{k-1}^e(\mathrm{P}) \text{ such that } \mathbf{curl}\,\boldsymbol{v} = 0 \Big\},$$

and using also (5.19) on each face,

$$\mathbf{curl}\,\Big(V_{k-1}^e(\mathrm{P})\Big) \equiv \Big\{ \boldsymbol{v} \in V_{k-1}^f(\mathrm{P}) \text{ such that } \operatorname{div}\boldsymbol{v} = 0 \Big\}.$$

9. Conclusions

We presented a variant of *nodal* and *edge* Serendipity spaces on polygonal elements and applied them to the numerical solution of a simple magnetostatic problem. These Virtual Element Spaces of different type can be used together in applications where an exact sequence is particularly convenient, together with commuting-diagram interpolation operators, as is definitely the case in electromagnetic problems.

In more details, we introduced new families of H^1-conforming and $H(\mathrm{rot})$-conforming polygonal elements that generalize the traditional Lagrange Finite Elements and the Nédélec edge elements (both of the first and of the second kind) to the case of general polygons. Possibly most important is the fact that the new elements are very robust with

respect to distortions, and so are their Serendipity variants (where many internal degrees of freedom are eliminated). Such a feature is already interesting in rather simple geometries (as, for instance, quadrilaterals) and will also prove to be particularly convenient when applied to the *faces* of a polyhedral decomposition.

Here we considered the use of these spaces for the discretization of Magnetostatic problems in two dimensions, following the variational formulation of Kikuchi. We proved stability and optimal error estimate, and we checked the performance (which turned out to be very good) with some academic numerical experiments.

The extension to more general Hodge–Laplace type operators in 2D would be immediate, and the extension to the 3D Magnetostatic problems (much more interesting from the practical point of view) is reasonably "at hand", and profits significantly of the use of the present spaces on faces (in particular for the use of their Serendipity version).

It would also be interesting to study the extension of these methods to problems where the dependence of $\boldsymbol{B}$ from $\boldsymbol{H}$ is nonlinear. For applications of the Virtual Element Methods to various other types of nonlinear problems we refer to [52,56–58].

Clearly much additional work is needed, but we hope that our friend Tinsley will like the pioneering aspects.

Acknowledgments

The first and third authors were partially supported by the European Research Council through the H2020 Consolidator Grant (grant no. 681162) CAVE – Challenges and Advancements in Virtual Elements. This support is gratefully acknowledged.

References

[1] L. Beirão da Veiga, F. Brezzi, A. Cangiani, G. Manzini, L.D. Marini, A. Russo, Basic principles of virtual element methods, Math. Models Methods Appl. Sci. 23 (1) (2013) 199–214.
[2] L. Beirão da Veiga, F. Brezzi, L.D. Marini, A. Russo, The hitchhiker's guide to the virtual element method, Math. Models Methods Appl. Sci. 24 (8) (2014) 1541–1573.
[3] L. Beirão da Veiga, F. Brezzi, L.D. Marini, A. Russo, $H(div)$ and $H(curl)$-conforming VEM, Numer. Math. 133 (2) (2016) 303–332.
[4] J. Hyman, M. Shashkov, Adjoint operators for the natural discretizations of the divergence, gradient and curl on logically rectangular grids, Appl. Numer. Math. 25 (4) (1997) 413–442.
[5] K. Lipnikov, G. Manzini, M. Shashkov, Mimetic finite difference method, J. Comput. Phys. 257 (part B) (2014) 1163–1227.
[6] L. Beirão da Veiga, K. Lipnikov, G. Manzini, The Mimetic Finite Difference Method for Elliptic Problems, in: MS&A. Modeling, Simulation and Applications, vol. 11, Springer-Verlag, 2014.
[7] F. Brezzi, A. Buffa, K. Lipnikov, Mimetic finite differences for elliptic problems, M2AN Math. Model. Numer. Anal. 43 (2) (2009) 277–295.
[8] L. Beirão da Veiga, K. Lipnikov, G. Manzini, Arbitrary-order nodal mimetic discretizations of elliptic problems on polygonal meshes, SIAM J. Numer. Anal. 49 (5) (2011) 1737–1760.
[9] D.N. Arnold, F. Brezzi, B. Cockburn, L.D. Marini, Unified analysis of discontinuous Galerkin methods for elliptic problems, SIAM J. Numer. Anal. 39 (5) (2001) 1749–1779.
[10] C.E. Baumann, T. Oden, A discontinuous hp finite element method for convection–diffusion problems, Comput. Methods Appl. Mech. Engrg. 175 (3–4) (1999) 311–341.
[11] B. Cockburn, Discontinuous Galerkin methods, ZAMM Z. Angew. Math. Mech. 83 (2003) 731–754.
[12] V. Dolejší, M. Feistauer, Discontinuous Galerkin method, in: Analysis and Applications to Compressible Flow, in: Springer Series in Computational Mathematics, vol. 48, Springer, Cham, 2015.
[13] B. Cockburn, J. Gopalakrishnan, R. Lazarov, Unified hybridization of discontinuous Galerkin, mixed, and continuous Galerkin methods for second order elliptic problems, SIAM J. Numer. Anal. 47 (2) (2009) 1319–1365.
[14] B. Cockburn, The hybridizable discontinuous Galerkin methods, in: Proceedings of the International Congress of Mathematicians. Vol. IV, Hindustan Book Agency, New Delhi, 2010, pp. 2749–2775.
[15] B. Cockburn, D. Di Pietro, A. Alexandre Ern, Bridging the hybrid high-order and hybridizable discontinuous galerkin methods, ESAIM Math. Model. Numer. Anal. 50 (2016) 635–650.
[16] E. Wachspress, Rational bases for convex polyhedra, Comput. Math. Appl. 59 (6) (2010) 1953–1956.
[17] L. Demkowicz, J.T. Oden, W. Rachowicz, O. Hardy, Toward a universal h-p adaptive finite element strategy 1 - Constrained approximation and data structure, Comput. Methods Appl. Mech. Engrg. 77 (1–2) (1989) 79–112.
[18] J.T. Oden, L. Demkowicz, W. Rachowicz, T.A. Westermann, Toward a universal h-p adaptive finite element strategy 2 - A posteriori error estimation, Comput. Methods Appl. Mech. Engrg. 77 (1–2) (1989) 113–180.
[19] W. Rachowicz, J.T. Oden, L. Demkowicz, Toward a universal h-p adaptive finite element strategy 3 - Design of h-p meshes, Comput. Methods Appl. Mech. Engrg. 77 (1–2) (1989) 181–212.
[20] M. Arroyo, M. Ortiz, Local maximum-entropy approximation schemes, in: Meshfree Methods for Partial Differential Equations III, in: Lect. Notes Comput. Sci. Eng., vol. 57, Springer, Berlin, 2007, pp. 1–16.
[21] M.S. Floater, Generalized barycentric coordinates and applications, Acta Numer. 24 (2015) 215–258.

[22] G. Manzini, A. Russo, N. Sukumar, New perspectives on polygonal and polyhedral finite element methods, Math. Models Methods Appl. Sci. 24 (8) (2014) 1665–1699.
[23] C.A. Duarte, I. Babuska, J.T. Oden, Generalized finite element methods for three-dimensional structural mechanics problems, Comput. & Structures 77 (2) (2000) 215–232.
[24] N. Sukumar, E.A. Malsch, Recent advances in the construction of polygonal finite element interpolants, Arch. Comput. Methods Eng. 13 (1) (2006) 129–163.
[25] J. Droniou, R. Eymard, T. Gallouët, R. Herbin, Gradient schemes: a generic framework for the discretisation of linear, nonlinear and nonlocal elliptic and parabolic equations, Math. Models Methods Appl. Sci. 23 (13) (2013) 2395–2432.
[26] P. Chow, M. Cross, K. Pericleous, A natural extension of the conventional finite volume method into polygonal unstructured meshes for CFD application, Appl. Math. Model. 20 (1996) 170–183.
[27] J. Droniou, R. Eymard, T. Gallouët, R. Herbin, A unified approach to mimetic finite difference, hybrid finite volume and mixed finite volume methods, Math. Models Methods Appl. Sci. 20 (2) (2010) 265–295.
[28] K. Lipnikov, D. Svyatskiy, Y. Vassilevski, Interpolation-free monotone finite volume method for diffusion equations on polygonal meshes, J. Comput. Phys. 228 (2009) 703–716.
[29] L. Beirão da Veiga, C. Lovadina, G. Vacca, Divergence free virtual elements for the Stokes problem on polygonal meshes, ESAIM Math. Model. Numer. Anal. 51 (2017) 509–535.
[30] E. Artioli, C. de Miranda, C. Lovadina, L. Patruno, A stress/displacement virtual element method for plane elasticity problems, Comput. Methods Appl. Mech. Engrg 325 (2017) 155–174.
[31] L. Beirão da Veiga, F. Brezzi, L.D. Marini, Virtual elements for linear elasticity problems, SIAM J. Numer. Anal. 51 (2) (2013) 794–812.
[32] M.F. Benedetto, S. Berrone, S. Pieraccini, S. Scialò, The virtual element method for discrete fracture network simulations, Comput. Methods Appl. Mech. Engrg. 280 (2014) 135–156.
[33] F. Brezzi, L.D. Marini, Virtual element methods for plate bending problems, Comput. Methods Appl. Mech. Engrg. 253 (2013) 455–462.
[34] A.L. Gain, C. Talischi, G.H. Paulino, On the virtual element method for three-dimensional linear elasticity problems on arbitrary polyhedral meshes, Comput. Methods Appl. Mech. Engrg. 282 (2014) 132–160.
[35] E. Cáceres, G.N. Gatica, A mixed virtual element method for the pseudostress-velocity formulation of the Stokes problem, IMA J. Numer. Anal. 37 (1) (2017) 296–331.
[36] I. Perugia, P. Pietra, A. Russo, A plane wave virtual element method for the Helmholtz problem, ESAIM Math. Model. Numer. Anal. 50 (3) (2016) 783–808.
[37] F. Kikuchi, Mixed formulations for finite element analysis of magnetostatic and electrostatic problems, Japan J. Appl. Math. 6 (1989) 209–221.
[38] H. Kanayama, R. Motoyama, K. Endo, F. Kikuchi, Three dimensional magnetostatic analysis using nedelec's elements, IEEE Trans. Magn. 26 (1990) 682–685.
[39] L. Beirão da Veiga, F. Brezzi, L.D. Marini, A. Russo, Serendipity nodal VEM spaces, Comput. Fluids 141 (2016) 2–12.
[40] L. Beirão da Veiga, F. Brezzi, L.D. Marini, A. Russo, Serendipity face and edge VEM spaces, Rend. Lincei Sci. Fis. Nat. 28 (1) (2017) 143–180.
[41] D.N. Arnold, D. Boffi, R.S. Falk, Approximation by quadrilateral finite elements, Math. Comp. 71 (239) (2002) 909–922.
[42] D.N. Arnold, D. Boffi, R.S. Falk, Quadrilateral $H(\mathrm{div})$ finite elements, SIAM J. Numer. Anal. 42 (6) (2005) 2429–2451.
[43] B. Ahmad, A. Alsaedi, F. Brezzi, L.D. Marini, A. Russo, Equivalent projectors for virtual element methods, Comput. Math. Appl. 66 (3) (2013) 376–391.
[44] F. Brezzi, R.S. Falk, L.D. Marini, Basic principles of mixed virtual element methods, ESAIM Math. Model. Numer. Anal. 48 (4) (2014) 1227–1240.
[45] D. Boffi, F. Brezzi, M. Fortin, Mixed Finite Element Methods and Applications, in: Springer Series in Computational Mathematics, vol. 44, Springer, Heidelberg, 2013.
[46] D.N. Arnold, R.S. Falk, R. Winther, Finite element exterior calculus, homological techniques, and applications, Acta Numer. 15 (2006) 1–155.
[47] L. Demkowicz, Computing with hp-Adaptive Finite Elements. Vol. 1. One and Two Dimensional Elliptic and Maxwell Problems, in: Applied Mathematics and Nonlinear Science, Chapman & Hall/CRC, Boca Raton, 2007.
[48] L. Demkowicz, J. Kurtz, D. Pardo, M. Paszenski, W. Rachowicz, A. Zdunek, Computing with hp-Adaptive Finite Elements. Vol. 2. Frontiers: Three Dimensional Elliptic and Maxwell Problems with Applications, in: Applied Mathematics and Nonlinear Science, Chapman & Hall/CRC, Boca Raton, 2008.
[49] P. Monk, Finite element methods for Maxwell's equations, in: Numerical Mathematics and Scientific Computation, Oxford University Press, New York, 2003.
[50] D. Boffi, Fortin operator and discrete compactness for edge elements, Numer. Math. 87 (2000) 229–246.
[51] D. Boffi, A note on the de Rham complex and a discrete compactness property, Appl. Math. Lett. 14 (2001) 33–38.
[52] P. Wriggers, W. Rust, B. Reddy, A virtual element method for contact, Comput. Mech. 58 (2016) 1039–1050.
[53] L. Beirão da Veiga, C. Lovadina, A. Russo, Stability analysis for the virtual element method, 2016. arXiv:1607.05988. (in press).
[54] S. Brenner, Q. Guan, L. Sung, Some estimates for virtual element methods, Comput. Methods Appl. Math. (2017). http://dx.doi.org/10.1515/cmam-2017-0008.
[55] L. Beirão da Veiga, D. Mora, G. Rivera, R. Rodríguez, A virtual element method for the acoustic vibration problem, Numer. Math. 136 (2017) 725–736.
[56] L. Beirão da Veiga, C. Lovadina, G. Vacca, Virtual Elements for the Navier-Stokes problem on polygonal meshes, 2017. arXiv:1703.00437, (submitted for publication).

[57] P.F. Antonietti, L. Beirão da Veiga, S. Scacchi, M. Verani, A C^1 virtual element method for the Cahn-Hilliard equation with polygonal meshes, SIAM J. Numer. Anal. 54 (1) (2016) 34–57.

[58] H. Chi, L.B. da Veiga, G. Paulino, Some basic formulations of the virtual element method (VEM) for finite deformations, Comput. Methods Appl. Mech. Engrg. 318 (2017) 148–192.